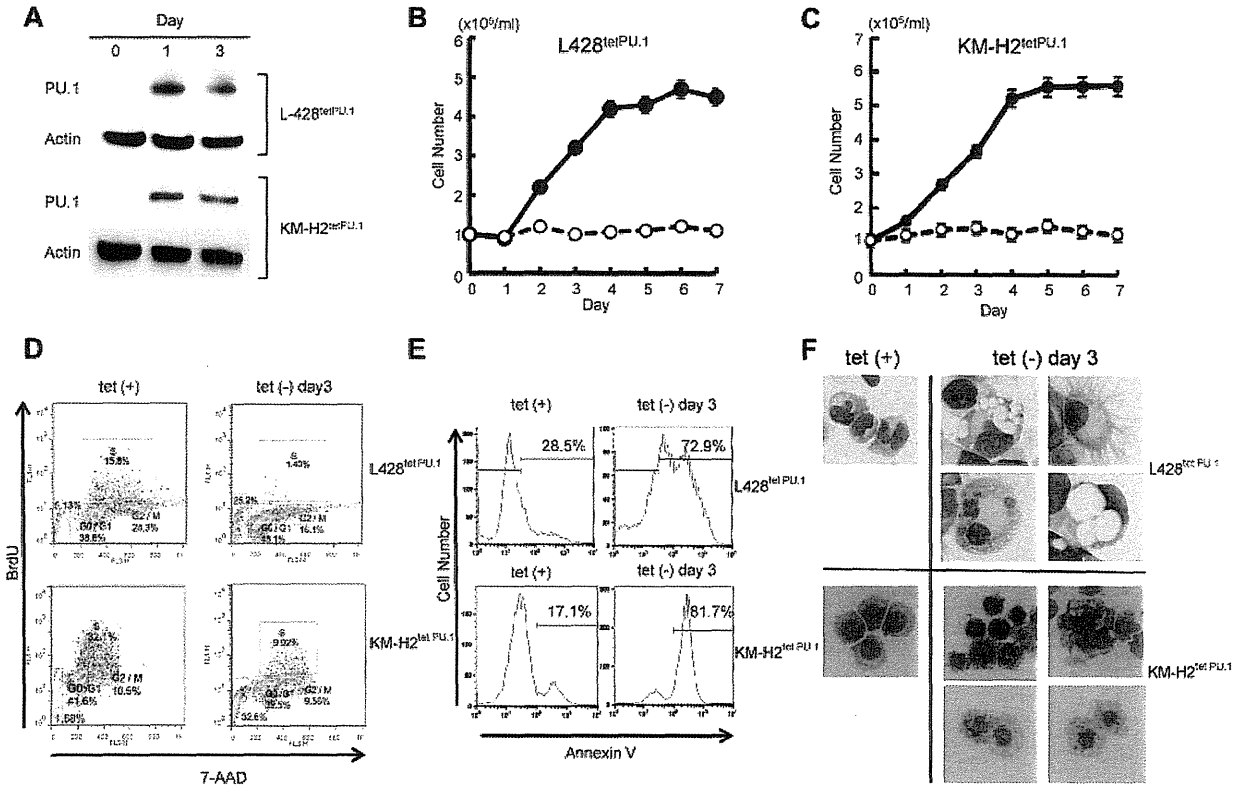

Figure 2. PU.1 induces growth arrest and apoptosis in L428 and KM-H2 cHL cell lines in vitro. (A) Western blot of PU.1 protein after tetracycline withdrawal. PU.1 was highly induced after tetracycline withdrawal in L428$^{tetPU.1}$ and KM-H2$^{tetPU.1}$ cells. PU.1 induced growth arrest in L428$^{tetPU.1}$ (B) and KM-H2$^{tetPU.1}$ cells (C) after tetracycline removal (○), whereas uninduced cells (●) grew comparably to wild-type parental cells. (D) Cell-cycle analysis was performed in L428$^{tetPU.1}$ and KM-H2$^{tetPU.1}$ cells by BrdU and 7-aminoactinomycin D staining. PU.1 induced G_1 arrest and led to a significant decrease in S-phase cells in L428$^{tetPU.1}$ and KM-H2$^{tetPU.1}$ cell lines. (E) PU.1 induced apoptosis in L428$^{tetPU.1}$ and KM-H2$^{tetPU.1}$ cells as assessed by annexin V staining. (F) PU.1 induced morphologic changes in L428$^{tetPU.1}$ and KM-H2$^{tetPU.1}$ cells. L428$^{tetPU.1}$ cells expressing PU.1 exhibited numerous different-sized cell processes and vacuoles compared with uninduced cells. A number of cells displayed nuclear fragmentation (Tet$^-$, day 3, bottom left panel). The majority of KM-H2$^{tetPU.1}$ cells expressing PU.1 also contained relatively small-sized vacuoles and nuclear condensation, indicative of apoptosis. Images were acquired using a BX60 microscope and DP70 digital camera with DP controller software (Olympus; ×400 magnification).

survival rate. In comparison, mice without tetracycline and harboring larger tumors tended to have skin ulcers at the site of the shrinking tumor and acquired lethal infections.

These data suggest that PU.1 may act as a tumor suppressor of cHL in vivo.

PU.1 induces apoptosis in primary cells purified from patients with Hodgkin lymphoma

Next, to evaluate whether PU.1 induces apoptosis of primary cHL cells, we purified lymphoma cells from the lymph nodes of patients with cHL. Negative selection was performed with anti-CD3, -CD14, -CD16, -CD19, -CD20, and -CD56 antibodies, and purified cells consisted of > 90% Hodgkin and Reed Sternberg-cells as confirmed by May-Giemsa staining of cytospin samples (Figure 4A). These cells were also CD30-positive as confirmed by flow cytometry or immunohistochemistry (supplemental Figure 1A-B, available on the *Blood* Web site; see the Supplemental Materials link at the top of the online article). After purification, primary Hodgkin lymphoma cells cultured alone survived for 1 day. However, coculture with cells obtained from patient lymph nodes prolonged survival to at least 3 days, as confirmed by microscopy of cytospin samples. Therefore, we infected cells obtained from whole lymph nodes, including Hodgkin cells, with lentivirus overexpressing human PU.1 or empty vector control. After 3 days in culture, primary Hodgkin lymphoma cells were purified by negative selection and subjected to annexin V staining. Cells transduced with lentivirus were recognized as Venus-positive cells and were analyzed by staining with propidium iodide (PI) and annexin V antibody. In case 1, overexpression of PU.1 led to a decrease in live cells (PI$^-$/annexin V$^-$) compared with empty vector (52.4% vs 69.8%), and a concomitant increase in PI$^-$/annexin V$^+$ preapoptotic cells (19.7% vs 8.6%; Figure 4B, left panel). In addition, primary cHL cells transduced with PU.1 exhibited various-sized vacuoles in cytosol (Figure 4A, right panels). In case 2, overexpression of PU.1 also led to a decrease in live cells (PI$^-$/annexin V$^-$) compared with control vector (9.4% vs 18.1%), and an increase in PI$^+$ apoptotic cells (PI$^+$/annexin V$^-$ and PI$^+$/annexin V$^+$) compared with vector only (81% vs 68%; Figure 4B, middle panel). In case 3, overexpression of PU.1 also led to a decrease in live cells (PI$^-$) compared with control vector (62.7% vs 92.1%) and an increase in PI$^+$ apoptotic cells (PI$^+$/annexin V$^-$ and PI$^+$/annexin V$^+$) compared with vector only (37.2% vs 17.9%; Figure 4B right panel). These experiments were performed in biologic duplicate with similar results. These data suggest that PU.1 also induces apoptosis in primary Hodgkin lymphoma cells.

Growth arrest of L428$^{tetPU.1}$ cells induced by PU.1 is at least partially dependent on up-regulation of p21

To elucidate the mechanisms underlying cell-cycle arrest and apoptosis induced by PU.1, we compared gene expression profiles

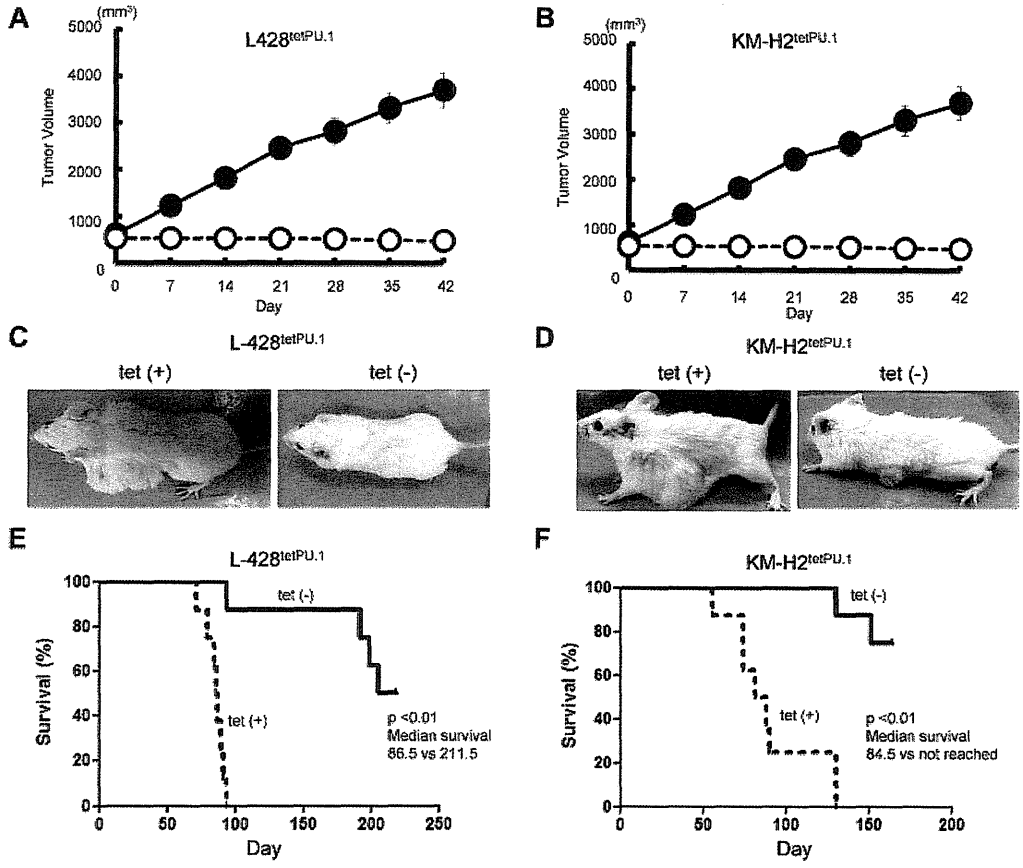

Figure 3. PU.1 induces growth arrest and apoptosis in both L428$^{tetPU.1}$ and KM-H2$^{tetPU.1}$ cHL cell lines in vivo. Tumor size in L428$^{tetPU.1}$ (A) and KM-H2$^{tetPU.1}$ (B) xenograft mouse models over the course of 7 days. Tumors in L428$^{tetPU.1}$ and KM-H2$^{tetPU.1}$ mice given tetracycline continued to grow (●), compared with tumors in mice without tetracycline, which ceased to grow and in some cases decreased in size (○). Tumors in L428$^{tetPU.1}$ (C) and KM-H2$^{tetPU.1}$ (D) xenografts did not grow after tetracycline withdrawal. Left panels: Tumors in a xenograft mouse taking tetracycline water. Right panel: Tumors after tetracycline withdrawal. Survival curves of L428$^{tetPU.1}$ (E) and KM-H2$^{tetPU.1}$ (F) xenograft mice. L428$^{tetPU.1}$ xenograft mice taking tetracycline all died within 96 days, whereas 7 of 8 mice without tetracycline survived > 190 days. KM-H2$^{tetPU.1}$ xenograft mice taking tetracycline all died within 143 days, whereas 6 of 8 mice without tetracycline survived > 155 days.

of L428$^{tetPU.1}$ and KM-H2$^{tetPU.1}$ cells 0, 1, and 3 days after PU.1 induction, by DNA microarray. In the case of L428$^{tetPU.1}$ cells, the top 30 genes up-regulated and down-regulated at day 1 and day 3 are shown in supplemental Tables 1 through 4. Genes up-regulated 24 hours after PU.1 induction (> 8-fold at day 1) are shown in Figure 5A. These genes contain IFN-stimulated genes (ISGs), including *TRIM22*, *IFI44L*, and *OAS3*. We previously reported that ISGs, including *IFIT1*, *IFITM1*, *IFIT2*, *IFIT4*, *IFI27*, *ISG15*, *LY6E*, and *IFI6*, were up-regulated in the multiple myeloma cell line, U266, after induction of PU.1 expression using the same tet-off system. IRF7, a key transcription factor involved in IFN signal transduction, was also highly up-regulated as previously shown in U266 cells expressing PU.1. Within the category of genes related to cell cycle or apoptosis, we observed that *p21 (CDKN1A)* was highly up-regulated at day 1 and day 3 after PU.1 induction, and this was confirmed by real-time PCR and Western blot (Figure 5B-C).

To clarify the role of p21 up-regulation in Hodgkin lymphoma cell growth, we stably silenced p21 in L428$^{tetPU.1}$ cells using siRNA. p21 siRNA strongly suppressed p21 expression in L428$^{tetPU.1}$ cells, before and after PU.1 induction (Figure 6A). Stable knockdown of p21 rescued L428$^{tetPU.1}$ cells from growth arrest induced by PU.1 (Figure 6B). Taken together, these data suggest that L428$^{tetPU.1}$ growth arrest induced by PU.1 is at least partially dependent on p21 up-regulation.

In the case of KM-H2$^{tetPU.1}$ cells, genes up-regulated after PU.1 induction (> 10-fold at day 1) are shown in supplemental Figure 2. The top 30 genes up-regulated and down-regulated one or 3 days after PU.1 induction are shown in supplemental Tables 5 through 8. *p21* was not included in these genes. Indeed, p21 was not up-regulated at the protein level after PU.1 induction, whereas *p21* mRNA was up-regulated 6-fold (Figure 5B-C). Therefore, the mechanisms underlying cell-cycle arrest in KH-M2$^{tetPU.1}$ cells expressing PU.1 may be distinct from those of L428$^{tetPU.1}$ cells expressing PU.1. There were no highly up-regulated ISGs; however, *IRF7* was highly up-regulated at both day 1 (13-fold) and day 3 (14.6-fold). Among genes related to the immune system, *IL1RN*, *LILRA3*, *IGDCC3*, and *LILRA2* were highly up-regulated both at day 1 and day 3. Within the category of genes related to cell cycle or apoptosis, *Aurora kinase C* and *FGFR4* were highly up-regulated one and 3 days after PU.1 induction. Among down-regulated genes that may be related to cell cycle or apoptosis, *PRDM1* and *TNFRSF18* were highly down-regulated at day 1 after PU.1 induction. Notably, PRDM1 is a key transcription factor involved in late B-cell differentiation; however, down-regulation of *PRDM1* was not sustained (0.9-fold) 3 days after PU.1 induction. Further studies are required to elucidate the role of these genes in cell-cycle arrest and apoptosis observed in KM-H2 $^{tetPU.1}$ cells after PU.1 induction.

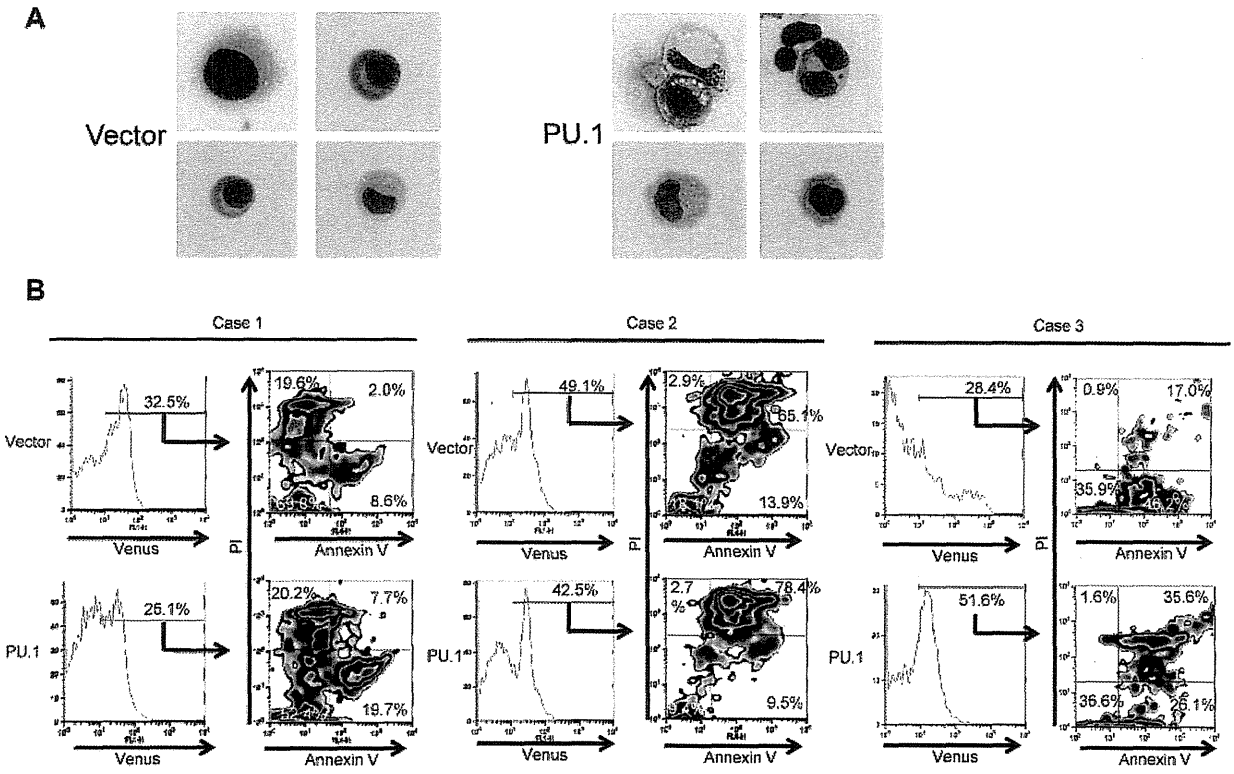

Figure 4. PU.1 induces apoptosis in primary cHL cells from patients. (A) Morphology of purified, primary cHL cells transduced with control lentivirus (Case 1, 4 left panels) or PU.1 expressing lentivirus (Case 1, 4 right panels). A number of primary classic Hodgkin cells expressing PU.1 contained various-sized vacuoles Images were acquired using a BX60 microscope and DP70 digital camera with DP controller software (Olympus; ×1000 magnification). (B) Primary cHL cells transduced with PU.1 lentivirus tended to undergo apoptosis compared with cells transduced with empty vector. Apoptosis was assessed in Venus-positive cells by flow cytometry after staining with PI and allophycocyanin-conjugated annexin V. Stable transduction of primary cHL cells from case 1 with PU.1 lentivirus led to a decrease in the percentage of live PI^-/annexin V^- cells and an increased percentage of PI^-/annexin V^+ preapoptotic cells, compared with control vector. Stable transduction of primary cHL cells from case 2 with PU.1 lentivirus also led to a decrease in the percentage of live PI^-/annexin V^- cells and an increased percentage of PI^+ apoptotic cells. Stable transduction of primary cHL cells from case 3 with PU.1 lentivirus also led to a decrease in the percentage of live PI^-/annexin V^+ cells and an increased percentage of PI^+ apoptotic cells.

5-aza-2′-deoxycytidine and/or trichostatin A induces up-regulation of PU.1 and apoptosis in cHL cells

Given that PU.1 is down-regulated in Hodgkin lymphoma cells by promoter and URE methylation, and that overexpression of PU.1 induced growth arrest and apoptosis of Hodgkin lymphoma cells, we hypothesized that up-regulation of PU.1 after treatment with demethylation agents and/or histone deacetylase (HDAC) inhibitors might represent a new therapeutic modality for Hodgkin lymphoma patients. We first evaluated the ability of 5-aza-2′-deoxycytidine to induce PU.1 expression. Treatment of Hodgkin lymphoma cell lines with 1μM 5-aza-2′-deoxycytidine induced *PU.1* mRNA expression in HD-70, L540, HDLM2, and KM-H2 cells but not in L428 cells (Figure 7A).

We next evaluated the ability of HDAC inhibitors to induce PU.1 expression. Whereas treatment with SAHA failed to induce *PU.1* expression in either L428, KM-H2 cells, trichostatin A induced expression of *PU.1* mRNA in KM-H2 cells, but not in L428 cells (data not shown). We also evaluated the effect of combined treatment with both 5-aza-2′-deoxycytidine and trichostatin A on cell growth and apoptosis in Hodgkin lymphoma cell lines. Treatment of L428 cells with 1μM 5-aza-2′-deoxycytidine and 500nM trichostatin A led to induction of *PU.1* mRNA expression (Figure 7A right panel). We next evaluated the effects of these agents on these Hodgkin lymphoma cell growth. Treatment with 1μM 5-aza-2′-deoxycytidine induced growth arrest in HD-70, L540, HDLM2, and KM-H2 cells (Figure 7B-E); however, L428 cells remained unaffected after treatment with 1μM 5-aza-2′-deoxycytidine (Figure 7F). In contrast, the combination of 1μM 5-aza-2′-deoxycytidine and 500nM trichostatin A induced growth arrest in L428 cells (Figure 7G). Given that the combination of 5-aza-2′-deoxycytidine and trichostatin A, but not treatment with 5-aza-2′-deoxycytidine alone, was capable of inducing PU.1 expression and growth arrest in L428 cells, these results indicate that PU.1 is at least partially responsible for inducing growth arrest of L428 cells in this setting. These data suggest that up-regulation of PU.1 by demethylation agents and HDAC inhibitors may represent a new therapeutic strategy for the treatment of cHL.

Discussion

In this study, we present data demonstrating that PU.1 is a potent tumor suppressor in cHL. First, using bisulfite sequencing, we showed that PU.1 is silenced by the methylation of its promoter and a −17 kb URE. Next, we demonstrated that PU.1 induced growth arrest and apoptosis in cHL cell lines, L428 and KM-H2, and primary cHL cells in vitro. In addition, using a xenograft mouse model harboring tumors of L428 or KM-H2 cells, we showed that PU.1 up-regulation induced tumor regression and promoted long-term survival, compared with mice without PU.1 induction. Finally, we showed that, in the case of L428 cells, growth arrest induced by PU.1 was mediated, at least in part, by the up-regulation of p21.

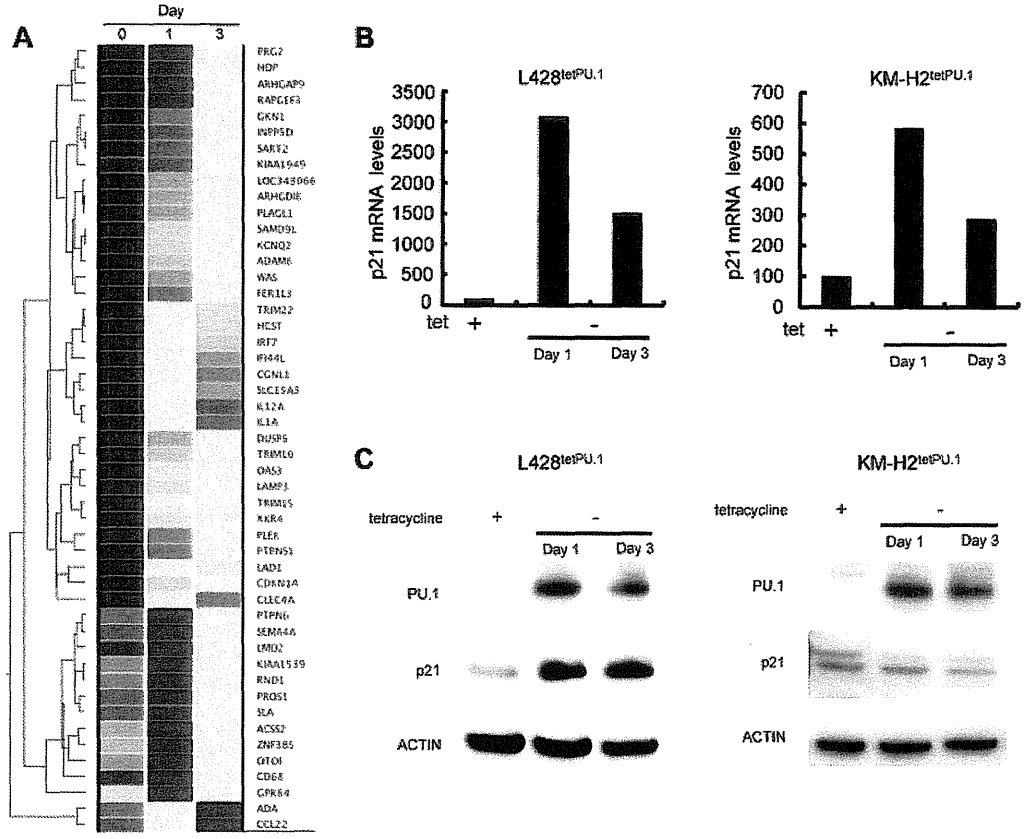

Figure 5. p21 is highly up-regulated in L428$^{tetPU.1}$ cells after PU.1 induction. (A) Heatmap of DNA microarray analysis comparing the gene expression profiles of L428$^{tetPU.1}$ cells after PU.1 induction at days 0, 1, and 3. *p21 (CDKN1A)* mRNA was highly up-regulated after PU.1 induction. (B) *p21* mRNA was up-regulated in both L428$^{tetPU.1}$ and KM-H2$^{tetPU.1}$ cells after PU.1 induction. Real-time PCR was performed 1 and 3 days after PU.1 induction. (C) p21 protein was up-regulated in L428$^{tetPU.1}$ but not in KM-H2$^{tetPU.1}$ cells after PU.1 induction. Western blot for p21, PU.1, and actin was performed 1 and 3 days after PU.1 induction.

The oncogenic mechanisms underlying cHL are not well understood. Many B cell–specific genes are down-regulated in cHL cells, including B cell–specific transcription factors, Oct2, Bob1, and PU.1, and cell surface markers, CD19, CD20, and CD79.[15] Down-regulation of these genes is caused by promoter methylation.[23] In contrast, cHL cells express CD30, a marker expressed on activated B cells and T cells. However, to date, the significance of the down-regulation of B cell–specific genes and the expression of CD30 in cHL remain enigmatic.

One of the genetic lesions of cHL is constitutive activation of the canonical nuclear factor of κ light polypeptide gene enhancer in B-cells (NF-κB) pathway.[37] A recent report showed that TNFAIP3 (A20), a negative regulator of the NFκB pathway, is inactivated by deletions and somatic mutations in 40% of cHL patients and in the cHL cell line, KM-H2.[13] In addition to TNFAIP3, somatic mutations of *NFκBIA*, which also inhibits the NF-κB signaling pathway, have been identified in KM-H2 cells.[37] *NFκBIA*, also known as IκB, is mutated in ~ 20% of cHL patients.[37-40] It is also well documented that ~ 50% of cHL patients harbor amplification or gain of *REL*, which is a component of NFκB.[41-43] Taken together, these data indicate that constitutive activation of NFκB is a key event underlying the pathogenesis of cHL. Our microarray analysis of L428$^{tetPU.1}$ cells revealed that PU.1 induced a 2- to 3-fold

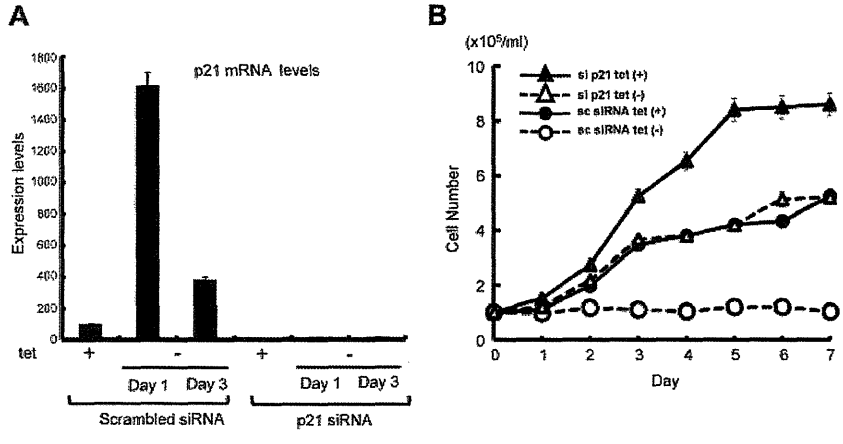

Figure 6. PU.1-induced cell growth arrest in L428$^{tetPU.1}$ cells is dependent on p21 up-regulation. (A) Stable knockdown of p21 strongly suppressed p21 expression, even after PU.1 induction in L428$^{tetPU.1}$ cells. (B) The growth arrest of L428$^{tetPU.1}$ cells induced by PU.1 overexpression was reversed by targeted knockdown of p21. PU.1-induced growth arrest in L428$^{tetPU.1}$ cells stably transduced with scrambled siRNA (○), whereas PU.1 failed to induce growth arrest in L428$^{tetPU.1}$ cells stably transduced with p21 siRNA (△).

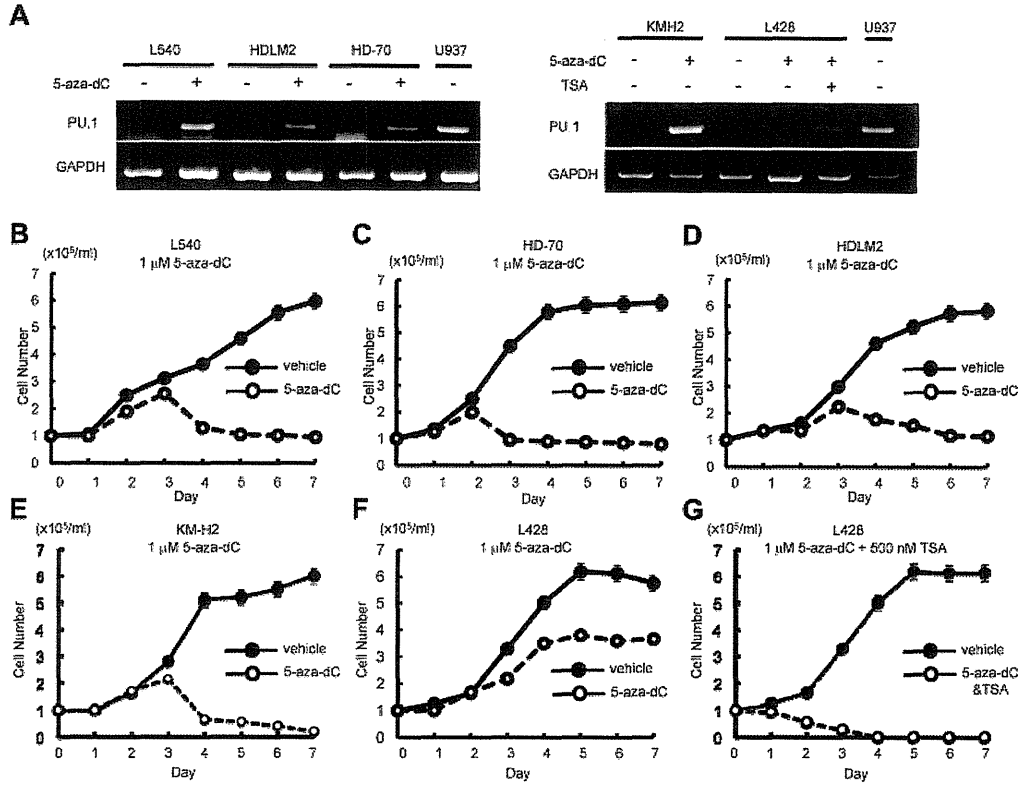

Figure 7. Individual or combined treatment with demethylation agent and HDAC inhibitors is a possible therapeutic strategy for cHL. (A) 5-aza-2′-deoxycytidine and/or trichostatin A (TSA) induced PU.1 expression in cHL cell lines. Treatment of L540, HDLM2, HD-70, and KM-H2 cells with 1 μM 5-aza-2′-deoxycytidine induced PU.1 expression after 3 days. In contrast, treatment of L428 cells with 1 μM 5-aza-2′-deoxycytidine failed to induce PU.1 expression, whereas the combined treatment with 1 μM 5-aza-2′-deoxycytidine and 500nM TSA led to induction of PU.1 expression after 3 days. (B-E) Treatment of L540 (B), HD-70 (C), HDLM2 (D), and KM-H2 (E) cells with 1 μM 5-aza-2′-deoxycytidine induced growth arrest. (F) Treatment of L428 cells with 1 μM 5-aza-2′-deoxycytidine failed to induce growth arrest. (G) The combined treatment of L428 cells with 1 μM 5-aza-2′-deoxycytidine and 500nM of TSA induced growth arrest.

up-regulation of TNFAIP3 at both 1 and 3 days (data not shown). Up-regulation of TNFAIP3 may block the NFκB pathway, therefore accounting for the observed cell-cycle arrest and apoptosis in L428 $^{tetPU.1}$ cells after PU.1 induction. In contrast, we did not observe any significant change in the expression of NFκB composite proteins (> 2-fold) in L428$^{tetPU.1}$ cells after PU.1 induction, indicating that PU.1 does not affect the expression of composite members of the NFκB protein complex.

In this study, we also elucidated the mechanisms of L428$^{tetPU.1}$ and KM-H2$^{tetPU.1}$ cell growth arrest after PU.1 induction. Gene expression profiling of L428$^{tetPU.1}$ cells after induction of PU.1 revealed up-regulation of p21, and this accounted at least in part for the cell growth arrest. These results are very similar to our previous finding that p21 is up-regulated by PU.1, leading to cell-cycle arrest in the U266 myeloma cell line.[27] Therefore, loss of p21 expression may be involved in the dysregulation of cell growth in some subsets of B-cell malignancies that have lost PU.1 expression. In contrast, the KM-H2 Hodgkin lymphoma cell line did not display p21 up-regulation at the protein level after PU.1 induction. Thus, up-regulation of p21 does not explain the growth arrest observed after PU.1 induction in all subsets of B-cell malignancies. In the case of apoptosis, we previously reported that PU.1 induces apoptosis in U266 myeloma cells via up-regulation of the TNF-related apoptosis inducing ligand.[27] Nevertheless, TNF-related apoptosis inducing ligand was intrinsically highly expressed in L428$^{tetPU.1}$ and KM-H2 $^{tetPU.1}$ cells in the absence of PU.1 expression, and PU.1 did not further induce TNF-related apoptosis inducing ligand expression in either cell line. Therefore, the mechanism of apoptosis induced by PU.1 in these Hodgkin lymphoma cell lines is probably different from that observed in U266 myeloma cells. The identification of downstream effector proteins involved in PU.1-induced apoptosis in cHL cells may therefore provide new molecular targets for therapy in these patients.

In conclusion, we show that up-regulation of PU.1 in cHL cells induces cell-cycle arrest and apoptosis in vitro and in vivo, and demonstrate that cell-cycle arrest is accounted for, at least partially, by up-regulation of p21. Based on these data, it is possible that demethylation agents and HDAC inhibitors, which induce PU.1 up-regulation, may represent new molecular target modalities for treatment of patients with cHL.

Acknowledgments

This work was supported by the Ministry of Education, Culture, Sports, Science and Technology of Japan.

Authorship

Contribution: H.Y. conducted the majority of experiments, generated KM-H2$^{tetPU.1}$ cells and the xenograft model mice, and wrote the manuscript; S.U. isolated mRNA for DNA microarray analysis; H.T. designed the project; S.E. performed lentiviral transduction and flow cytometry; Y. Kawano analyzed survival curves of xenograft mice; H.N., T.I., and K.A. performed DNA microarray

analysis; Y. Komohara and M.T. performed immunostaining of primary Hodgkin lymphoma cells; H.H., T.W., and H.M. gave useful advice; S.O. generated *Rag2*$^{-/-}$*Jak3*$^{-/-}$ *balb/c* mice and gave useful advice to generate xenograft mice; and Y.O. designed the project, generated L428$^{tetPU.1}$ cells, and wrote manuscript.

Conflict-of-interest disclosure: The authors declare no competing financial interests.

Correspondence: Yutaka Okuno, Department of Hematology, Kumamoto University of Medicine, 1-1-1 Honjo, Kumamoto 860-8556, Japan; e-mail: yokuno@gpo.kumamoto-u.ac.jp.

References

1. Chan J, Jaffe E, Ralfkiaer E, Ko Y. *WHO Classification of Tumours of Haematopoietic and Lymphoid Tissues*. 4th Ed. Lyon, France: IARC Press; 2008.
2. Meyer RM, Gospodarowicz MK, Connors JM, et al. ABVD alone versus radiation-based therapy in limited-stage Hodgkin's lymphoma. *N Engl J Med*. 2012;366(5):399-408.
3. von Tresckow B, Plutschow A, Fuchs M, et al. Dose-intensification in early unfavorable Hodgkin's lymphoma: final analysis of the German Hodgkin Study Group HD14 Trial. *J Clin Oncol*. 2012;30(9):907-913.
4. Viviani S, Zinzani PL, Rambaldi A, et al. ABVD versus BEACOPP for Hodgkin's lymphoma when high-dose salvage is planned. *N Engl J Med*. 2011;365(3):203-212.
5. Chisesi T, Bellei M, Luminari S, et al. Long-term follow-up analysis of HD9601 trial comparing ABVD versus Stanford V versus MOPP/EBV/CAD in patients with newly diagnosed advanced-stage Hodgkin's lymphoma: a study from the Intergruppo Italiano Linfomi. *J Clin Oncol*. 2011; 29(32):4227-4233.
6. Borchmann P, Haverkamp H, Diehl V, et al. Eight cycles of escalated-dose BEACOPP compared with four cycles of escalated-dose BEACOPP followed by four cycles of baseline-dose BEACOPP with or without radiotherapy in patients with advanced-stage Hodgkin's lymphoma: final analysis of the HD12 trial of the German Hodgkin Study Group. *J Clin Oncol*. 2011;29(32):4234-4242.
7. Halbsguth T, Nogova L, Mueller H, et al. Phase 2 study of BACOPP (bleomycin, adriamycin, cyclophosphamide, vincristine, procarbazine, and prednisone) in older patients with Hodgkin lymphoma: a report from the German Hodgkin Study Group (GHSG). *Blood*. 2010;116(12):2026-2032.
8. Eich H, Diehl V, Gorgen H, et al. Intensified chemotherapy and dose-reduced involved-field radiotherapy in patients with early unfavorable Hodgkin's lymphoma: final analysis of the German Hodgkin Study Group HD11 trial. *J Clin Oncol*. 2010;28(27):4199-4206.
9. Engert A, Diehl V, Franklin J, et al. Escalated-dose BEACOPP in the treatment of patients with advanced-stage Hodgkin's lymphoma: 10 years of follow-up of the GHSG HD9 study. *J Clin Oncol*. 2009;27(27):4548-4554.
10. Engert A, Plutschow A, Eich HT, et al. Reduced treatment intensity in patients with early-stage Hodgkin's lymphoma. *N Engl J Med*. 2010; 363(7):640-652.
11. van der Kaaij MA, Heutte N, Meijnders P, et al. Premature ovarian failure and fertility in long-term survivors of Hodgkin's lymphoma: a European Organisation for Research and Treatment of Cancer Lymphoma Group and Groupe d'Etude des Lymphomes de l'Adulte Cohort Study. *J Clin Oncol*. 2012;30(3):291-299.
12. Swerdlow AJ, Higgins CD, Smith P, et al. Second cancer risk after chemotherapy for Hodgkin's lymphoma: a collaborative British cohort study. *J Clin Oncol*. 2011;29(31):4096-4104.
13. Kato M, Sanada M, Kato I, et al. Frequent inactivation of A20 in B-cell lymphomas. *Nature*. 2009; 459(7247):712-716.
14. Jundt F, Kley K, Anagnostopoulos I, et al. Loss of PU.1 expression is associated with defective immunoglobulin transcription in Hodgkin and Reed-Sternberg cells of classical Hodgkin disease. *Blood*. 2002;99(8):3060-3062.
15. McCune R, Syrbu S, Vasef M. Expression profiling of transcription factors Pax-5, Oct-1, Oct-2, BOB. 1, and PU.1 in Hodgkin's and non-Hodgkin's lymphomas: a comparative study using high throughput tissue microarrays. *Mod Pathol*. 2006; 19(7):1010-1018.
16. Scott EW, Simon MC, Anastasi J, Singh H. Requirement of transcription factor PU.1 in the development of multiple hematopoietic lineages. *Science*. 1994;265(5178):1573-1577.
17. McKercher SR, Torbett BE, Anderson KL, et al. Targeted disruption of the PU.1 gene results in multiple hematopoietic abnormalities. *EMBO J*. 1996;15(20):5647-5658.
18. Li Y, Okuno Y, Zhang P, et al. Regulation of the PU.1 gene by distal elements. *Blood*. 2001; 98(10):2958-2965.
19. Okuno Y, Huang G, Rosenbauer F, et al. Potential autoregulation of transcription factor PU.1 by an upstream regulatory element. *Mol Cell Biol*. 2005; 25(7):2832-2845.
20. Tatetsu H, Ueno S, Hata H, et al. Down-regulation of PU.1 by methylation of distal regulatory elements and the promoter is required for myeloma cell growth. *Cancer Res*. 2007;67(11):5328-5336.
21. Rosenbauer F, Wagner K, Kutok JL, et al. Acute myeloid leukemia induced by graded reduction of a lineage-specific transcription factor, PU.1. *Nat Genet*. 2004;36(6):624-630.
22. Rosenbauer F, Owens BM, Yu L, et al. Lymphoid cell growth and transformation are suppressed by a key regulatory element of the gene encoding PU.1. *Nat Genet*. 2006;38(1):27-37.
23. Ushmorov A, Leithauser F, Sakk O, et al. Epigenetic processes play a major role in B-cell-specific gene silencing in classical Hodgkin lymphoma. *Blood*. 2006;107(6):2493-2500.
24. Era T, Witte ON. Regulated expression of P210 Bcr-Abl during embryonic stem cell differentiation stimulates multipotential progenitor expansion and myeloid cell fate. *Proc Natl Acad Sci U S A*. 2000;97(4):1737-1742.
25. Miyoshi H, Takahashi M, Gage FH, Verma IM. Stable and efficient gene transfer into the retina using an HIV-based lentiviral vector. *Proc Natl Acad Sci U S A*. 1997;94(19):10319-10323.
26. Miyoshi H, Blomer U, Takahashi M, Gage FH, Verma IM. Development of a self-inactivating lentivirus vector. *J Virol*. 1998;72(10):8150-8157.
27. Ueno S, Tatetsu H, Hata H, et al. PU.1 induces apoptosis in myeloma cells through direct transactivation of TRAIL. *Oncogene*. 2009;28(46): 4116-4125.
28. Dolbeare F, Gratzner H, Pallavicini MG, Gray JW. Flow cytometric measurement of total DNA content and incorporated bromodeoxyuridine. *Proc Natl Acad Sci U S A*. 1983;80(18):5573-5577.
29. Peterson KR, Clegg CH, Huxley C, et al. Transgenic mice containing a 248-kb yeast artificial chromosome carrying the human beta-globin locus display proper developmental control of human globin genes. *Proc Natl Acad Sci U S A*. 1993;90(16):7593-7597.
30. Kaufman RM, Pham CT, Ley TJ. Transgenic analysis of a 100-kb human beta-globin cluster-containing DNA fragment propagated as a bacterial artificial chromosome. *Blood*. 1999;94(9): 3178-3184.
31. Tanimoto K, Liu Q, Bungert J, Engel JD. Effects of altered gene order or orientation of the locus control region on human beta-globin gene expression in mice. *Nature*. 1999;398(6725):344-348.
32. Yu W, Misulovin Z, Suh H, et al. Coordinate regulation of RAG1 and RAG2 by cell type-specific DNA elements 5′ of RAG2. *Science*. 1999; 285(5430):1080-1084.
33. Loots GG, Locksley RM, Blankespoor CM, et al. Identification of a coordinate regulator of interleukins 4, 13, and 5 by cross-species sequence comparisons. *Science*. 2000;288(5463):136-140.
34. Okuno Y, Iwasaki H, Huettner CS, et al. Differential regulation of the human and murine CD34 genes in hematopoietic stem cells. *Proc Natl Acad Sci U S A*. 2002;99(9):6246-6251.
35. Okuno Y, Huettner CS, Radomska HS, et al. Distal elements are critical for human CD34 expression in vivo. *Blood*. 2002;100(13):4420-4426.
36. Radomska HS, Gonzalez DA, Okuno Y, et al. Transgenic targeting with regulatory elements of the human CD34 gene. *Blood*. 2002;100(13): 4410-4419.
37. Kuppers R. The biology of Hodgkin's lymphoma. *Nat Rev Cancer*. 2009;9(1):15-27.
38. Cabannes E, Khan G, Aillet F, Jarrett R, Hay R. Mutations in the IkBa gene in Hodgkin's disease suggest a tumour suppressor role for IkappaBalpha. *Oncogene*. 1999;18(20):3063-3070.
39. Emmerich F, Meiser M, Hummel M, et al. Overexpression of I kappa B alpha without inhibition of NF-kappaB activity and mutations in the I kappa B alpha gene in Reed-Sternberg cells. *Blood*. 1999;94(9):3129-3134.
40. Jungnickel B, Staratschek-Jox A, Brauninger A, et al. Clonal deleterious mutations in the IkappaBalpha gene in the malignant cells in Hodgkin's lymphoma. *J Exp Med*. 2000;191(2):395-402.
41. Barth T, Martin-Subero J, Joos S, et al. Gains of 2p involving the REL locus correlate with nuclear c-Rel protein accumulation in neoplastic cells of classical Hodgkin lymphoma. *Blood*. 2003;101(9): 3681-3686.
42. Joos S, Menz C, Wrobel G, et al. Classical Hodgkin lymphoma is characterized by recurrent copy number gains of the short arm of chromosome 2. *Blood*. 2002;99(4):1381-1387.
43. Martin-Subero J, Gesk S, Harder L, et al. Recurrent involvement of the REL and BCL11A loci in classical Hodgkin lymphoma. *Blood*. 2002;99(4): 1474-1477.

The EMBO Journal (2012) 31, 2994–3007 | © 2012 European Molecular Biology Organization | All Rights Reserved 0261-4189/12
www.embojournal.org

THE EMBO JOURNAL

Chd2 interacts with H3.3 to determine myogenic cell fate

Akihito Harada[1], Seiji Okada[1], Daijiro Konno[2], Jun Odawara[1], Tomohiko Yoshimi[3], Saori Yoshimura[3], Hiromi Kumamaru[1], Hirokazu Saiwai[1], Toshiaki Tsubota[4], Hitoshi Kurumizaka[5], Koichi Akashi[6], Taro Tachibana[3], Anthony N Imbalzano[7] and Yasuyuki Ohkawa[1,*]

[1]Department of Advanced Medical Initiatives, JST-CREST, Faculty of Medicine, Kyushu University, Fukuoka, Japan, [2]Laboratory for Cell Asymmetry, Center for Developmental Biology, RIKEN, Kobe, Japan, [3]Department of Bioengineering, Graduate School of Engineering, Osaka City University, Osaka, Japan, [4]Experimental Research Center for Infectious Diseases, Institute for Virus Research, Kyoto University, Kyoto, Japan, [5]Laboratory of Structural Biology, Graduate School of Advanced Science and Engineering, Waseda University, Tokyo, Japan, [6]Department of Medicine and Biosystemic Science, Faculty of Medicine, Kyushu University, Fukuoka, Japan and [7]Department of Cell Biology, University of Massachusetts Medical School, Worcester, MA, USA

Cell differentiation is mediated by lineage-determining transcription factors. We show that chromodomain helicase DNA-binding domain 2 (Chd2), a SNF2 chromatin remodelling enzyme family member, interacts with MyoD and myogenic gene regulatory sequences to specifically mark these loci via deposition of the histone variant H3.3 prior to cell differentiation. Directed and genome-wide analysis of endogenous H3.3 incorporation demonstrates that knockdown of Chd2 prevents H3.3 deposition at differentiation-dependent, but not housekeeping, genes and inhibits myogenic gene activation. The data indicate that MyoD determines cell fate and facilitates differentiation-dependent gene expression through Chd2-dependent deposition of H3.3 at myogenic loci prior to differentiation.
The EMBO Journal (2012) **31**, 2994–3007. doi:10.1038/emboj.2012.136; Published online 8 May 2012
Subject Categories: chromatin & transcription; differentiation & death
Keywords: chromatin; differentiation; histone variant; myogenesis

Introduction

The mechanisms by which a lineage-committed but undifferentiated cell maintains the ability to specifically activate the appropriate differentiation programme upon differentiation signalling is poorly understood. Activation of differentiation-specific genes depends on the binding of lineage-determining transcription factors to specific regulatory regions and on the appropriate regulation of chromatin structure. Hence, the future gene expression pattern of the differentiated cell must be present in the chromatin structure of the undifferentiated cell in the form of some sort of marking of the genome. However, how this marking is established and recognized is not clear.

To elucidate the mechanism of this marking of the whole genome, extensive study of chromatin structure in relation to cell differentiation has been undertaken. For example, methylation of specific DNA sequences by DNA methyltransferase activity is required for mouse development (Okano *et al*, 1999). It has also been reported that maintenance of histone modifications in the respective promoters of the HNF-1, HNF-4 and albumin genes through the cell cycle in hepatocytes facilitates expression of these genes (Kouskouti and Talianidis, 2005). Moreover, examination of histone acetylation levels in embryonic stem (ES) cells indicates hyperacetylation of histones H3 and H4 in the undifferentiated state (Meshorer *et al*, 2006). In fact, gene expression patterns are marked from an early stage for the maintenance of differentiation. Recently, characteristic histone variants have been identified that mark the active and the inactive state (Hake *et al*, 2006). For example, H3.3 has been found to be enriched with active H3K4me2/3, H3K9Ac and H3K14Ac marks and to be predominantly incorporated in the regulatory regions of transcriptionally active genes (Wirbelauer *et al*, 2005). In contrast, H3.2 is enriched with repressive H3K27me2/3 and H3K9me2 marks (Hake *et al*, 2006; Garcia *et al*, 2007). Therefore, exchange of histone variants is involved in the appropriate switching on and off of genes. In mouse ES cells, H3.3 is found at many developmental regulatory genes that are 'bivalent genes', marked with transcription-repressing H3K27me and transcription-activating H3K4me3 (Goldberg *et al*, 2010). In addition, over-expression of H3.3 results in maintenance of the transcriptionally active pattern of gene expression in specific tissue (Ng and Gurdon, 2008). These findings show that replacement of the histone variant (such as H3.3) contributes to the determination of selective gene expression, likely before histone modification (Hake and Allis, 2006).

Induction of transcriptional factors is also a method of controlling gene expression. For example, the myogenic transcription factor MyoD induces myogenic differentiation and can even promote reprogramming from a non-muscle cell to a muscle cell (Davis *et al*, 1987). A similar phenomenon is observed by introduction of specific lineage-determining regulators such as PPARγ2, or the four transcription factors that regulate formation of the induced pluripotent stem cell (Tontonoz *et al*, 1994; Takahashi and Yamanaka, 2006). Therefore, these transcription factors are required for reprogramming and alteration of the genomic state. It is known that these transcription factors regulate chromatin structure; to date, histone modification and chromatin remodelling have been identified as resultant changes, but a relationship between transcription factors and the type of

*Corresponding author. Department of Advanced Medical Initiatives, JST-CREST, Faculty of Medicine, Kyushu University, 3-1-1 Maidashi, Fukuoka 812-8582, Japan. Tel.: +81 92 642 6216; Fax: +81 92 642 6099; E-mail: yohkawa@epigenetics.med.kyushu-u.ac.jp

Received: 6 October 2011; accepted: 18 April 2012; published online: 8 May 2012

histone variant (such as incorporation of H3.3) has not been recorded.

MyoD is expressed in committed but undifferentiated cells, but how MyoD identifies genes for activation during differentiation is unknown. We hypothesized that a chromatin modifying or remodelling enzyme was likely involved. We identified chromodomain helicase DNA-binding domain 2 (Chd2), a member of the SNF2 family of chromatin remodelling enzymes, as a MyoD-interacting protein that facilitates cell fate determination via marking of myogenic genes by incorporation of the variant histone H3.3.

Results

Chd2 interacts with MyoD

It was previously shown that MyoD associates with Brg1, an enzyme of the mammalian SWI/SNF class of ATP-dependent chromatin remodelers, in differentiating muscle cells (Simone *et al*, 2004; de la Serna *et al*, 2005). We theorized that chromatin remodelling enzymes also might interact with MyoD in undifferentiated cells. Using monoclonal antibodies we had generated against Brg1, Brm, Chd1, and Chd2 (Ohkawa *et al*, 2009; Okada *et al*, 2009; Harada *et al*, 2010b; Yoshimura *et al*, 2010), we identified Chd2, but not Brg1 or Brm, as a MyoD co-immunoprecipitation (co-IP) product in C2C12 myoblasts (Figure 1A; Supplementary Figure S1A). The closely related protein Chd1 (60% homology) was not co-immunoprecipitated with MyoD. Reciprocal co-IP confirmed that Chd2 interacted with MyoD (Figure 1A). Additionally a proximity ligation assay (PLA) was used to demonstrate interaction between Chd2 and MyoD. Interactions between Chd2 and MyoD were observed in both myoblasts and differentiated cells (Figure 1B). As a control, we examined interactions between MyoD and Brg1, which as expected, were greatly enhanced in differentiated cells (Figure 1C). Immunocytochemistry revealed that a subset of Chd2 and MyoD, both of which are exclusively nuclear, were co-localized prior to cell differentiation (Supplementary Figure S1B). A cross-correlation analysis (vanSteensel *et al*, 1996) of confocal images of Chd2 and MyoD provided further support for co-localization in myoblasts as well as in differentiated C2C12 cells, suggesting that the MyoD–Chd2 interaction persists during differentiation (Supplementary Figure S1B). The specificity of the MyoD–Chd2 association was further assessed by examining co-localization between MyoD and Chd1. Whereas 35–40% of the MyoD co-localized with Chd2 in both myoblast and myotube nuclei, only 7–15% of the MyoD co-localized with Chd1 (Supplementary Figure S1C). Chd2 protein levels were not significantly different in myoblasts and in differentiated cells (Figure 1D).

Chd2 binds to myogenic gene promoters

Chromatin IP (ChIP) was used to analyse whether Chd2 is localized at differentiation-dependent myogenic genes. Because Chd2 was identified as a MyoD-interacting protein, we focused on regulatory sequences containing E-boxes. Chd2 interacted with the promoters of numerous myogenic gene loci in undifferentiated as well as differentiated C2C12 cells but not with housekeeping genes such as *Gapdh* or the inactive *Igh* enhancer (Figure 2A; Supplementary Figure S1D). To examine whether Chd2 recruitment was dependent on MyoD, we performed ChIP assays in NIH3T3 cells directed to undergo myogenesis by ectopic expression of MyoD (Davis *et al*, 1987). We observed MyoD-dependent binding of Chd2 specifically at myogenic gene promoters but not at housekeeping or silent gene promoters (Figure 2B). Coincident binding of MyoD at these same myogenic sequences was confirmed (Supplementary Figure S1E). Western blot analysis showed that the expression of MyoD in these cells did not alter Chd2 levels (Figure 2C). In addition, MyoD levels in these cells were not over-expressed relative to MyoD expression in C2C12 cells (Supplementary Figure S1F).

To further demonstrate that Chd2 recruitment is MyoD-dependent, we reduced the expression of MyoD in C2C12 cells by siRNA treatment and observed that Chd2 binding to myogenic genes did not occur (Figure 2D). Western blot analysis confirmed that MyoD protein levels were reduced by the siRNA treatment and that Chd2 protein levels were not

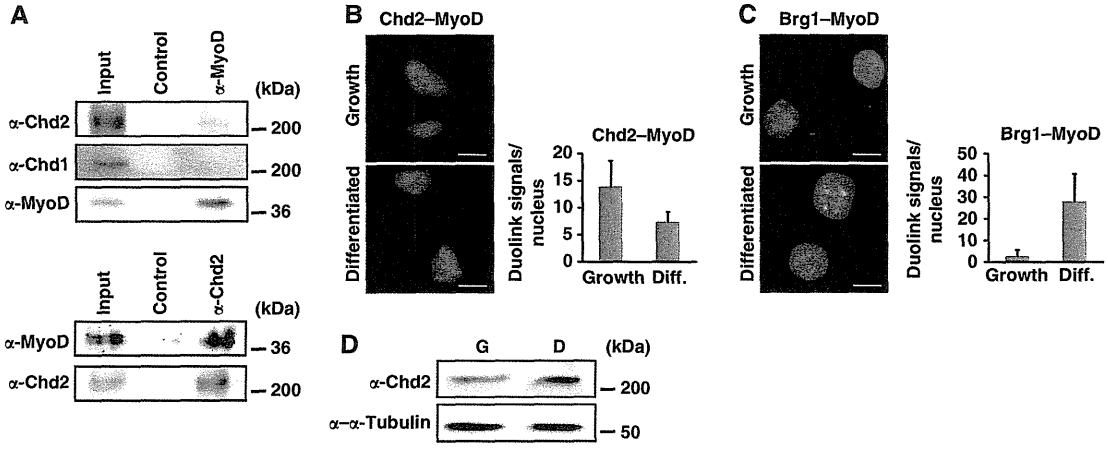

Figure 1 Chd2 interacts with MyoD. (**A**) Reciprocal IPs were performed from C2C12 myoblast extracts using MyoD- and Chd2-specific antibodies or IgG as a control. (**B**) PLAs indicating interaction of MyoD and Chd2 in both proliferating myoblasts and differentiated cells, in contrast to (**C**) the differentiation-specific interactions of MyoD and Brg1. Quantification represents the mean of three independent experiments, each of which analysed at least three separate fields ± s.d. Scale bars = 12.5 μm. (**D**) Western blot analysis of Chd2 levels in C2C12 cells under growth (G) or differentiation (D) conditions.

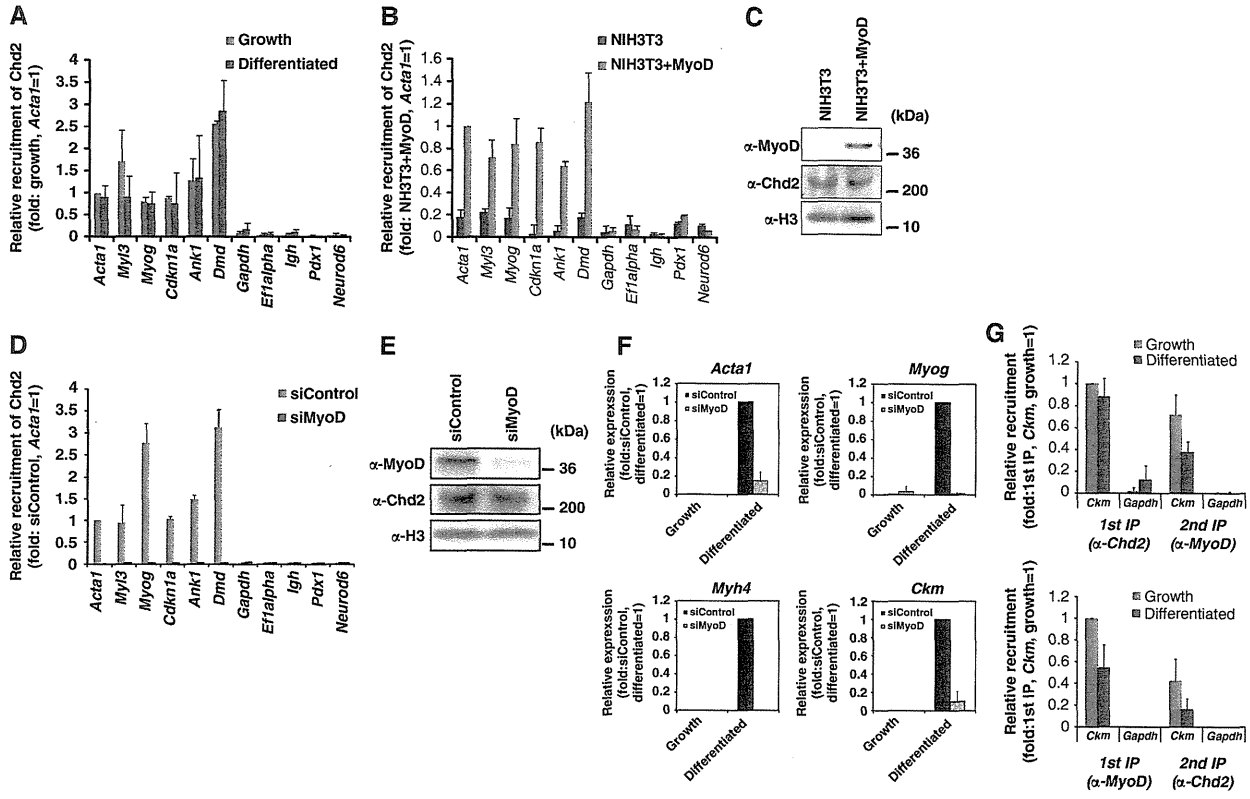

Figure 2 Chd2 interacts with MyoD and myogenic gene regulatory sequences. (**A**) ChIP assays for Chd2 binding at differentiation-dependent and skeletal muscle-specific (*Acta1*, *Myl3*, *Myog*, *Cdkn1a*, *Ank1*, *Dmd*), housekeeping (*Gapdh*, *Ef1alpha*), and silent (*IgH* enhancer, *Pdx1*, *Neurod6*) gene promoters were performed in C2C12 cells under growth and differentiated conditions. Relative recruitment was defined as the ratio of amplification of the PCR product relative to 1% of input genomic DNA. Values obtained from *Acta1* at the growth stage were defined as 1 and all other values were expressed relative to that value. Each value was standardized by the amplification efficiency of each primer pair. Quantification represents the mean of three independent experiments ± s.d. (**B**) Ectopic expression of MyoD induces Chd2 recruitment onto the promoter regions of myogenic genes. ChIP assays were performed as in (**A**) in fibroblast cells expressing MyoD or empty vector that were subjected to the differentiation protocol. (**C**) Western blot analysis for MyoD and Chd2 expression in MyoD-infected fibroblasts. H3 levels were monitored as a control. (**D**) siRNA-mediated MyoD knockdown inhibits Chd2 recruitment onto the promoter regions of myogenic genes. ChIP assays for Chd2 binding were performed as described in (**A**) in C2C12 myoblasts treated with either control siRNA or MyoD siRNA. (**E**) siRNA-mediated knockdown of the endogenous MyoD protein in C2C12 cells. A western blot analysis of C2C12 cells treated with either control siRNA or MyoD siRNA using antibodies against MyoD, Chd2, and H3 is shown. (**F**) Relative expression of skeletal muscle marker genes was reduced in C2C12 cells treated with MyoD siRNA. The levels of the indicated mRNAs were analysed by Q-PCR. The values in the differentiated cells expressing control siRNA were set to 1. Data represent the average of three independent experiments ± s.d. (**G**) Chd2 and MyoD co-recruitment at the *Ckm* but not the *Gapdh* promoter is shown by re-ChIP. Re-ChIP experiments sequentially used antibodies against Chd2 and MyoD, as indicated. Relative recruitment was defined as the ratio of amplification of the PCR product relative to 1% of input genomic DNA. Values obtained from *Ckm* at the growth stage with 1st IP were defined as 1 and all other values were expressed relative to that value. Each value was standardized by the amplification efficiency of each primer pair. Quantification represents the mean of three independent experiments ± s.d.

affected (Figure 2E). As expected, siRNA-mediated reduction of MyoD also compromised differentiation-dependent myogenic gene activation (Figure 2F). We then performed re-ChIP assays (Ohkawa *et al*, 2006). In C2C12 myoblasts maintained in growth media, Chd2 was simultaneously present with MyoD on the *Ckm* promoter but not on the *Gapdh* locus (Figure 2G). In differentiated C2C12 cells, Chd2 and MyoD were both present at the *Ckm* locus, but to a somewhat lesser extent than in myoblasts (Figure 2G). Collectively, these data strongly suggest that Chd2 is targeted to the *Ckm* promoter via MyoD and are consistent with results demonstrating widespread MyoD binding to myogenic genes in undifferentiated myoblasts (Cao *et al*, 2010).

Chd2 promotes myogenic gene expression

To explore the requirement for Chd2 in myogenesis, we suppressed Chd2 expression by stably introducing two microRNAs (miRNA) that target *Chd2* ($Chd2^{miR3139}$ and $Chd2^{miR5111}$) in C2C12 cells. We used cells stably transfected with *lacZ*-targeted miRNA ($Chd2^{WT}$) as a control. To indirectly monitor miRNA expression, enhanced green fluorescent protein—nuclear localization signal (EGFP–NLS) was expressed co-cistronically with the miRNA (Figure 3A). Analysis of myogenic gene expression in these cells indicated that myosin heavy chain expression, which is a late myogenic marker, was completely suppressed in both $Chd2^{miR3139}$ and $Chd2^{miR5111}$-expressing cells ($n=70$ and 63 GFP-positive cells, respectively; Figure 3A). The expression of myogenin, which is a marker of the early phase of myogenesis, was decreased in both cell lines to 6% ($Chd2^{miR3139}$, $n=109$ GFP-positive cells) and 13% of wild-type (WT) ($Chd2^{miR5111}$, $n=76$ GFP-positive cells; Figure 3A). Moreover, myotube formation was not observed in either miRNA-expressing cell line upon differentiation. Compared with controls, the mRNA

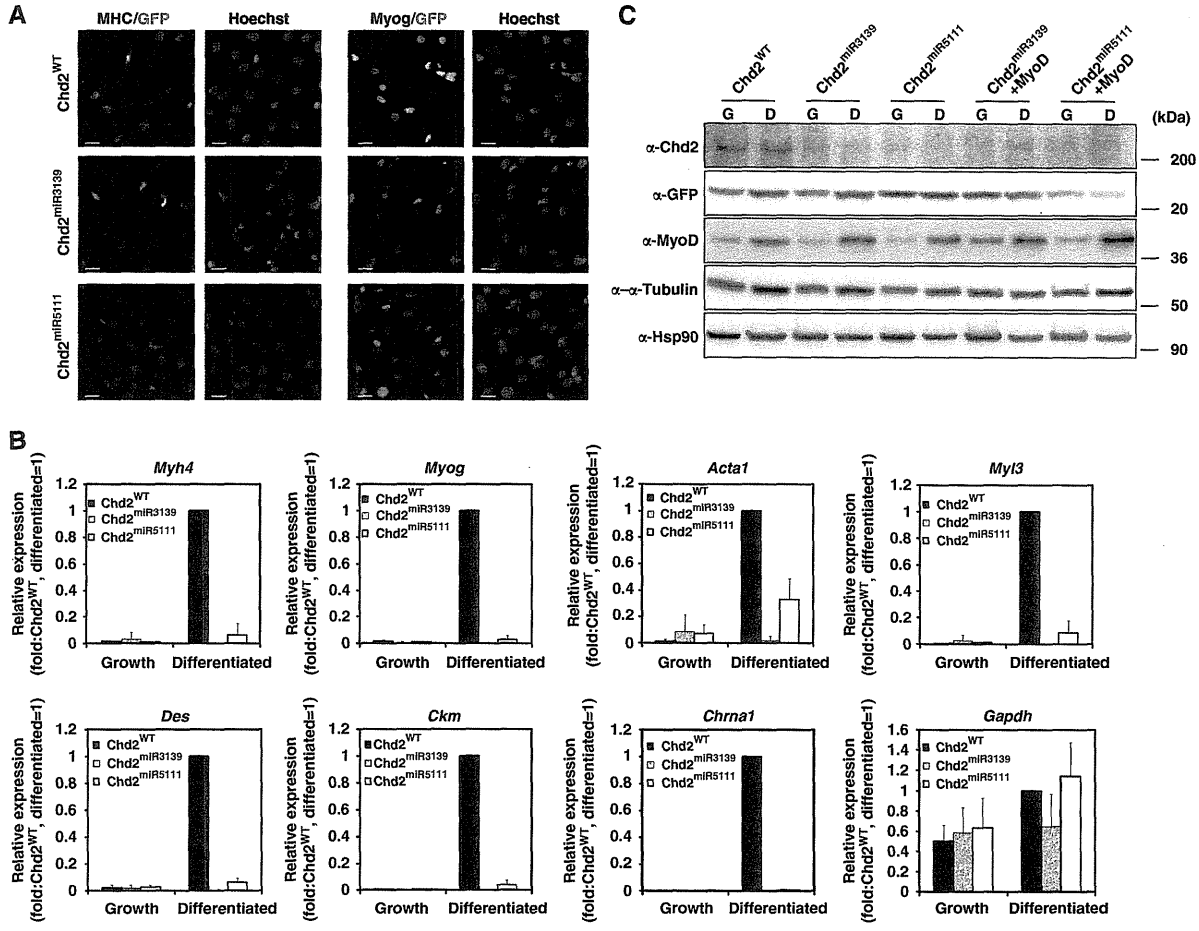

Figure 3 Chd2 is required for skeletal muscle differentiation. (**A**) The expression of myogenin (Myog) and myosin heavy chain (MHC) was not induced in C2C12 cells when Chd2 expression was suppressed by miRNAs targeting *Chd2*. To indirectly monitor miRNA expression, EGFP-NLS (EGFP fused with a nuclear transport signal) was expressed co-cistronically with miRNA. Scale bars = 5 μm. (**B**) The transcription of skeletal muscle marker genes was suppressed in C2C12 cells expressing miRNA targeting Chd2. mRNA levels were analysed by Q-PCR; data represent the average of three independent experiments ± s.d. *Gapdh* levels are shown as a control. (**C**) Western blot evaluating Chd2 protein knockdown and the expression of MyoD and other indicated proteins.

expression levels of every differentiation-dependent myogenic gene tested was significantly repressed in $Chd2^{miR3139}$ and $Chd2^{miR5111}$-expressing cells (Figure 3B). In contrast, expression of the housekeeping gene, *Gapdh*, was unaffected (Figure 3B).

Control experiments determined that *Chd2* transcript levels were not affected in cells expressing the Chd2-targeting miRNAs (Supplementary Figure S2A), but Chd2 protein expression was repressed (Figure 3C). This suggests that the specific miRNAs functioned as translational repressors of Chd2. The GFP expression level remained consistent, suggesting no significant differences in miRNA expression between the cells (Figure 3C). In addition, no significant differences in the expression of MyoD were observed between $Chd2^{WT}$ and miRNA-expressing cells, indicating that Chd2 was not regulating the expression of MyoD (Figure 3C). To confirm that changes in MyoD levels observed during differentiation did not alter Chd2 expression, we ectopically expressed MyoD in the Chd2 miRNA-expressing cells and showed that Chd2 expression (Figure 3C) and differentiation-dependent gene expression (Supplementary Figure S2B) were not rescued. We also determined that cell-cycle progression was not affected by miRNA expression in undifferentiated or differentiated cells as measured by FACS analysis (Supplementary Figure S2C) and western blot analysis of cyclins A and E (Supplementary Figure S2D). These data indicate that Chd2 is not indirectly affecting myogenic gene expression via alteration of cell-cycle arrest.

To complement these studies showing a requirement for Chd2 in myogenic differentiation, we reduced Chd2 expression by introducing siRNA molecules that target Chd2. siRNA-treated cells did not form myotubes as demonstrated by MHC staining (Supplementary Figure S3A) and were compromised for differentiation-specific gene expression (Supplementary Figure S3B). Western analysis demonstrated the reduction in Chd2 levels in siRNA-treated cells and no effect on MyoD levels (Supplementary Figure S3C).

To further confirm a Chd2-specific function in myogenic gene induction, we rescued the inhibition of *Chd2* expression by miRNA via the exogenous introduction of competitive mRNA fragments (*Chd2*-3011-3283 or *Chd2*-5004-5177) that were linked to the monomeric Kusabira Orange (mKO1) fluorescent protein containing a nuclear localization signal (Karasawa *et al*, 2004). In differentiated cells expressing

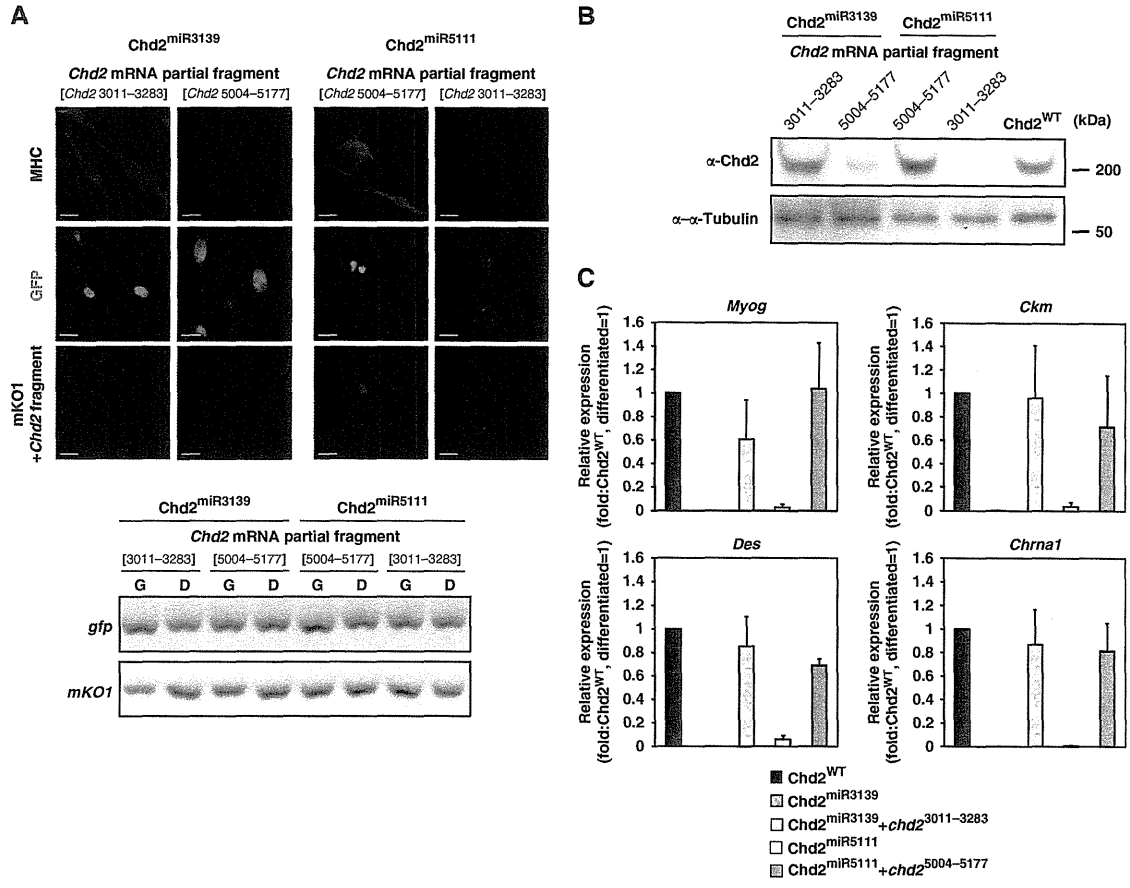

Figure 4 Myogenic phenotype is rescued by a forced expression of *Chd2* partial mRNA in Chd2 knockdown cells. (**A**) The expression of myosin heavy chain (MHC; blue) was re-induced in C2C12 cells expressing miRNAs targeting *Chd2* and a *Chd2* partial mRNA that competes each miRNA. To indirectly monitor miRNA and *Chd2* partial mRNA expression, EGFP–NLS (EGFP fused with a nuclear transport signal) and mKO1–NLS (mKO1 fused with a nuclear transport signal) were expressed co-cistronically with the miRNA and *Chd2* partial mRNA, respectively. Scale bars = 5 μm. Q-PCR analysis confirms equivalent expression of GFP and mKO1 in each sample (lower panel). (**B**) Chd2 expression was rescued in C2C12 cells expressing miRNAs targeting *Chd2* and the competing *Chd2* partial mRNA. Western blot analysis utilized antibodies against Chd2 and α-tubulin. (**C**) The transcription of skeletal muscle marker genes was rescued in C2C12 cells expressing miRNAs targeting *Chd2* and the competing *Chd2* partial mRNA. The levels of the indicated mRNAs were analysed by Q-PCR; data represent the average of three independent experiments ± s.d.

$Chd2^{miR3139}$, introduction of a competitive mRNA (*Chd2*-3011-3283) but not an mRNA from a different region of *Chd2* (*Chd2*-5004-5177), restored MHC expression (Figure 4A). Similarly, introduction of the mRNA (*Chd2*-5004-5177) rescued MHC expression in $Chd2^{miR5111}$-treated cells whereas introduction of the (*Chd2*-3011-3283) mRNA did not (Figure 4A). mKO1 expression levels were monitored to confirm equal expression of the competitive mRNAs in the cells (Figure 4A). Furthermore, under conditions where MHC expression was restored, we observed restoration of Chd2 protein levels (Figure 4B) and expression of *Myog*, *Ckm*, *Des*, and *Chrna1* at levels comparable to WT (Figure 4C).

As a complement to this set of experiments, we attempted to rescue the miRNA-mediated inhibition of *Chd2* expression and the inhibition of myogenesis via the exogenous introduction of full-length Chd2 cDNA or a Chd2 deletion mutant (Chd2-chromodomain deletion Δ-281–512 aa). Chromodomains facilitate interaction of proteins with chromatin via interaction with methylated histones (Pray-Grant *et al*, 2005). The constructs utilized were Flag-tagged and co-expressed the monomeric Kusabira Orange 2 (mKO2) fluorescent protein (Karasawa *et al*, 2004; Sakaue-Sawano *et al*, 2008). In differentiated cells expressing either $Chd2^{miR3139}$ or $Chd2^{miR5111}$, introduction of full-length Chd2 restored MHC expression and myotube formation, whereas expression of the Chd2 mutant lacking the chromodomain did not (Supplementary Figure S4A). Similarly, introduction of the full-length, but not the mutant Chd2, restored expression of *Acta1*, *Myog*, *Ckm*, and *Myh4* to levels comparable to those expressed in the control cells (Supplementary Figure S4B). Under conditions where myogenic gene expression and differentiation were restored, we observed restoration of Chd2 protein levels (Supplementary Figure S4C).

Chd2 interacts with histone H3.3

Since we observed that Chd2 was present at differentiation-dependent genes in proliferating myoblasts, we wished to address whether Chd2 might facilitate myogenic gene activation prior to the onset of differentiation and myogenic gene expression. CHD1, a related member of the CHD family, incorporates H3.3 into the nucleosome (Konev *et al*, 2007). H3.3 is a variant of H3 that is incorporated at

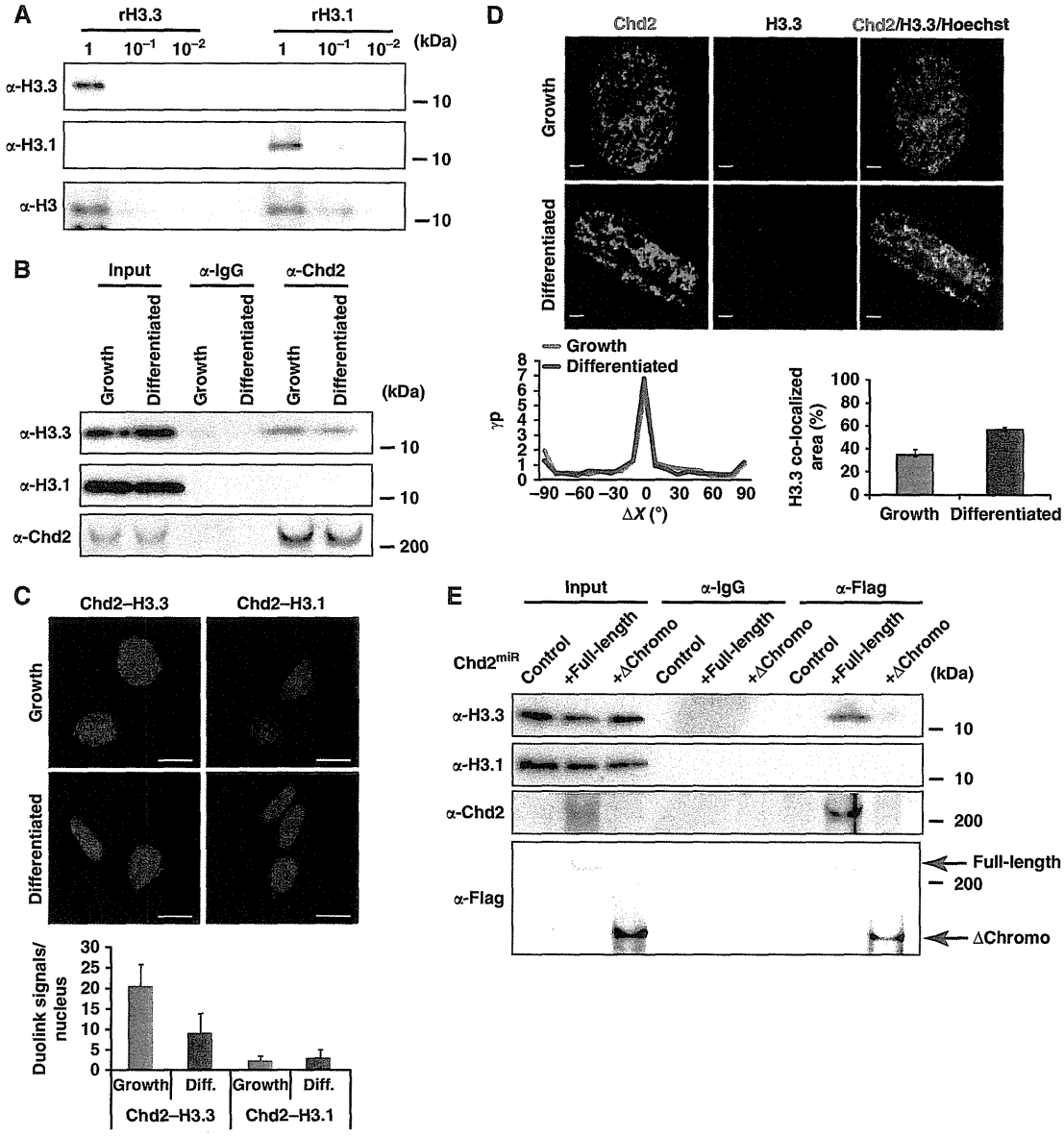

Figure 5 Chd2 interacts with H3.3 prior to and during skeletal muscle differentiation. (**A**) H3.3 antibody specifically discriminates between H3.3 and H3.1. Serial dilutions of purified recombinant H3.1 and H3.3 protein were evaluated by immunoblotting using the H3.3 and H3.1 monoclonal antibodies and the H3 polyclonal antibody. Detection of H3.3, H3.1, and H3 was performed on the same membrane. (**B**) IP from C2C12 cells using control IgG or Chd2-specific antibodies shows an interaction between Chd2 and H3.3. (**C**) PLAs indicating the frequency of interaction between H3.3 and Chd2 and between H3.1 and Chd2 in both proliferating myoblasts and differentiated cells. Quantification represents the mean of three independent experiments, each of which analysed at least three separate fields ± s.d. Scale bars = 12.5 μm. (**D**) C2C12 cells at growth and differentiated stages were immunostained with antibodies to Chd2 (green) and H3.3 (red) to show Chd2 and H3.3 co-localization. Confocal images, cross-correlation analysis, and the amount of H3.3 interacting with Chd2 are shown. Scale bars = 1 μm. (**E**) Co-immunoprecipitation from Chd2^{miR3139} cells expressing full-length Chd2–Flag or Chd2 deletion mutant (ΔChromodomain (281–512 aa)–Flag) using control IgG or Flag-antibodies shows an interaction between full-length Chd2 and H3.3.

transcriptionally activated genes (Ahmad and Henikoff, 2002; Jin *et al*, 2009). To evaluate whether Chd2 interacts with endogenous H3.3, we generated monoclonal antibodies to specifically distinguish H3.3 from H3.1, the major H3 isoform. H3.3 differs from H3.1 at only five residues, only one of which is in the N-terminal tail (position 31). Peptides spanning amino acids 21–39 were used as antigen. The specificity of each antibody was demonstrated by specific recognition of the appropriate recombinant H3.3 or H3.1 protein (Figure 5A). Specificity of the H3.3 antibody was further demonstrated by its specific recognition of modified and unmodified H3.3 and H3.1 peptides (Supplementary Figure S5A). Epitope mapping with recombinant H3.3 and H3.1 proteins revealed that the H3.3 antibody specifically recognized the unique S31 residue present in H3.3 (Supplementary Figure S5B). Since H3.3 is primarily associated with active transcription, we performed immunostaining to gauge the extent to which the H3.3 antibody recognizes euchromatin and heterochromatin, which is marked by intense Hoechst staining. The data indicate that the H3.3

antibody primarily recognizes euchromatic regions of the genome (Supplementary Figure S5C). This result is consistent with previous work showing that exogenous H3.3 is predominantly incorporated into active gene loci (Ahmad and Henikoff, 2002; Jin *et al*, 2009). Previously, H3.3 has been found to be enriched with active H3K4me2/3 marks, but not H3K9me2 marks (Wirbelauer *et al*, 2005; Hake *et al*, 2006; Garcia *et al*, 2007). Use of the H3.3 antibody in co-localization analyses with either H3K4me3 or H3K9me3 demonstrated significant co-localization with H3K4me3 but not H3K9me3 (Supplementary Figure S5D). Collectively, the data indicate that the H3.3 antibody specifically recognizes endogenous H3.3. We also determined that neither the overall nor the chromatin-associated levels of H3.3 changed as a function of C2C12 cell differentiation (Supplementary Figure S5E). Subsequent experiments showed that Chd2 could co-immunoprecipitate with H3.3, but not H3.1, in undifferentiated cells (Figure 5B). PLA assays also indicated Chd2–H3.3 interactions in myoblasts as well as differentiated cells, whereas the frequency of Chd2–H3.1 interactions was much lower (Figure 5C). Immuno-localization studies indicated Chd2–H3.3 co-localization in both undifferentiated and differentiated cells (Figure 5D). We further analysed the Chd2 and H3.3 interaction by co-IP using $Chd2^{mir3139}$ cells that exogenously express either Flag-tagged full-length Chd2 or the chromodomain deleted Chd2 mutant. Flag-tagged full-length Chd2 was immunoprecipitated with endogenous H3.3, while the Chd2 mutant was not (Figure 5E). Collectively, these studies suggest a possible link between Chd2 function and H3.3.

Chd2 mediates H3.3 incorporation into the regulatory regions of myogenic genes prior to the onset of myogenic gene expression

ChIP assays showed that H3.3 was incorporated at both myogenic and housekeeping gene regulatory sequences, including *Gapdh*, and *Ef1alpha*, but not at silent gene loci such as *Igh*, *Pdx1*, or *Neurod6* both in myoblasts and in differentiated cells (Figure 6A). This indicates that H3.3 marks myogenic genes prior to their expression. To confirm that H3.3 in fact was incorporated prior to the expression of these genes, duplicate plates were harvested for RNA. Q-PCR evaluation of myogenic gene expression demonstrated that the myoblast samples that showed H3.3 incorporation into myogenic gene promoters were not expressing myogenic genes (Supplementary Figure S6).

We next demonstrated that H3.3 is incorporated into the regulatory regions of myogenic genes in a Chd2-dependent manner. Relative incorporation of H3.3 in $Chd2^{miR}$ ($Chd2^{miR3139}$) expressing cells was decreased in the promoter regions of each of the myogenic genes in the undifferentiated state, but Chd2 knockdown had no effect on H3.3 incorporation at the *Gapdh* and *Ef1alpha* promoters (Figure 6B). H3.3 protein levels were the same in control and in miRNA-expressing cells before and after differentiation (Figure 6C). Therefore, H3.3 expression is regulated in a Chd2-independent manner. We further evaluated whether H3.3 incorporation into myogenic gene loci was MyoD-dependent. Introduction of MyoD into fibroblast cells preferentially induced H3.3 incorporation at myogenic genes without affecting H3.3 incorporation at housekeeping or silent gene loci (Figure 6D). Similarly, knockdown of MyoD in C2C12 myoblasts prevented H3.3 incorporation at myogenic, but not housekeeping genes (Figure 6E). In summary, H3.3 incorporation at myogenic genes occurs prior to differentiation and prior to myogenic gene expression in a Chd2- and MyoD-dependent manner.

Genome-wide analysis of H3.3 incorporation has been performed in HeLa and in ES cells using epitope-tagged H3.3 (Jin *et al*, 2009; Goldberg *et al*, 2010). We attempted ChIP-seq using the H3.3 antibody to evaluate the distribution of endogenous H3.3 and the Chd2 dependency of H3.3 deposition over the whole myoblast genome. First, the regions where H3.3 was incorporated in each chromosome were analysed by Boxplot. Total incorporation of H3.3 was almost equal in each chromosome in $Chd2^{WT}$ cells, with an average of about 0.63% (Figure 7A), showing that endogenous H3.3 is incorporated into a limited region of the genome. In contrast, the percentage of H3.3-incorporating regions in $Chd2^{miR3139}$ cells was decreased to about 0.27%. The fact that incorporation of H3.3 was not completely eliminated likely reflects the fact that H3.3 is also incorporated into the genome by other factors such as Hira and Chd1 (Ray-Gallet *et al*, 2002; Konev *et al*, 2007). The entire length of every annotated gene was defined as 1 and the levels of H3.3 incorporation at all gene loci were plotted (Supplementary Figure S7A). The results showed H3.3 incorporation at the transcription start sites (TSS), the transcription end sites (TES) and throughout the gene body. Interestingly, Chd2 reduction affected the incorporation of H3.3 at the TSS at a genome-wide level (Supplementary Figure S7A). These data differ from previous reports where H3.3 was localized immediately upstream of the TSS in HeLa cells (Jin *et al*, 2009; Goldberg *et al*, 2010) and was depleted from the TSS in ES cells (Jin *et al*, 2009; Goldberg *et al*, 2010), suggesting that H3.3 deposition in the vicinity of TSS may be cell-type specific.

To evaluate whether the genome marking derived from incorporation of H3.3 by Chd2 occurred at differentiation-specific genes, we analysed incorporation of H3.3 into the TSS relative to sequences immediately upstream and downstream at genes that were reported to be upregulated during C2C12 differentiation (Tomczak *et al*, 2004) (Supplementary Dataset 1). Analysis of H3.3 incorporation at differentiation-induced genes in $Chd2^{WT}$ cells indicated that H3.3 is significantly enriched around the TSS of the skeletal muscle-specific genes ($n = 545$) compared with enrichment in $Chd2^{miR}$-expressing cells (Figure 7B). In cells expressing Chd2-targeting miRNAs, we noted that a significant percentage of the genes showed no H3.3 incorporation while others showed reduced levels. A small percentage of genes showed redistribution of H3.3 (Figure 7B) within the locus, suggesting that Chd2 is required for deposition of H3.3 at the appropriate regions of myogenic gene loci.

Comparison of myogenic, housekeeping, and silent (Supplementary Dataset 1) genes showed that H3.3 incorporation at myogenic genes was dependent on Chd2 in the TSS region whereas incorporation at housekeeping genes was modestly affected by Chd2 knockdown (Figure 7C). Housekeeping genes were defined as those that are highly expressed in C2C12 cells 2 days before and 10 days after differentiation and were also expressed in NIH3T3 cells as previously reported (Berenjeno *et al*, 2007). Silent genes were defined as the genes that were only expressed in RAW264.7

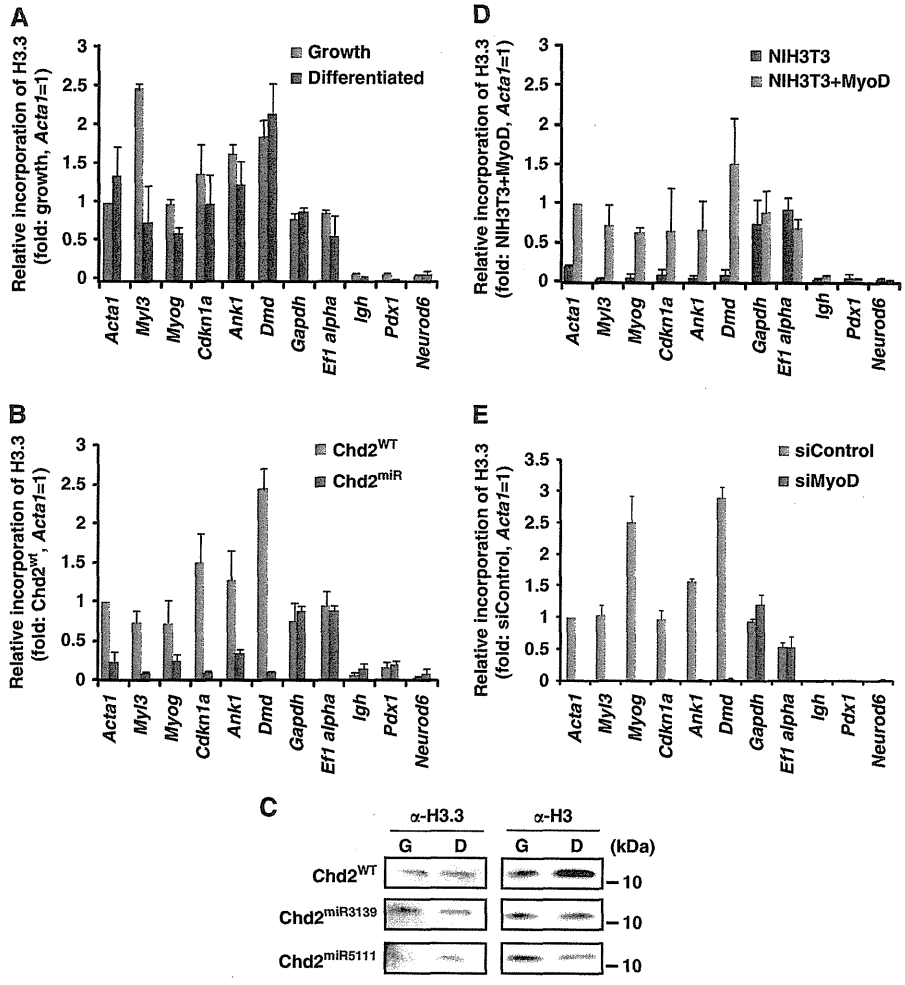

Figure 6 H3.3 incorporation at myogenic promoters occurs prior to differentiation and myogenic gene expression and is dependent on Chd2. (**A**) H3.3 incorporation at differentiation-specific myogenic gene promoters occurred prior to C2C12 cell differentiation. ChIP assays for myogenic, housekeeping, and silent genes were performed as described in Figure 2A. (**B**) Incorporation of H3.3 into myogenic gene loci is Chd2-dependent while incorporation housekeeping genes is Chd2-independent. ChIP assays for myogenic, housekeeping, and silent genes were in $Chd2^{WT}$ and $Chd2^{miR}$ ($Chd2^{miR3139}$) expressing C2C12 cells under growth conditions as described in Figure 2A. (**C**) $Chd2^{WT}$, $Chd2^{miR3139}$, and $Chd2^{miR5111}$-expressing C2C12 cells were cultured in growth medium for 1 day (G) and then shifted to differentiation medium for 48 h (**D**). H3.3 and total H3 expression levels were analysed by immunoblotting. (**D**) Ectopic expression of MyoD induces H3.3 incorporation at the promoter regions of myogenic genes. ChIP assays were performed as in Figure 2 in fibroblast cells expressing MyoD or empty vector. (**E**) siRNA-mediated MyoD knockdown inhibits H3.3 recruitment onto the promoter regions of myogenic, but not housekeeping, genes. ChIP assays were performed as in Figure 2 in C2C12 cells treated with either control siRNA or MyoD siRNA.

cells as previously reported (Covert *et al*, 2009) but not in C2C12 cells or in NIH3T3 cells. Silent genes were devoid of H3.3, but reduction of Chd2 levels caused a small number of genes to incorporate H3.3 around the TSS (Figure 7C). We then examined sequences at the transcriptional end sites (TES) region, which demonstrated that H3.3 incorporation at myogenic genes was enriched at the TES in a Chd2-dependent manner (Figure 7D). For reasons that are not understood, reduction of Chd2 levels increased H3.3 incorporation at sequences upstream of housekeeping gene TES but not at the TES itself, whereas silent genes were devoid of H3.3 at the TES (Figure 7D). We confirmed enrichment of H3.3 at the TSS and TES of the same set of myogenic genes in a different cell culture model for myogenesis. Exogenous expression of MyoD in NIH3T3 fibroblasts selectively induced H3.3 incorporation at the TSS and TES regions of muscle-specific genes relative to incorporation of H3.3 at these genes in mock-treated fibroblasts (Figure 7E). This result also demonstrates the MyoD dependency of H3.3 incorporation at myogenic loci. Finally, because the data indicated that Chd2 are incorporated at myogenic genes prior to differentiation and gene expression, we directly compared H3.3 incorporation across muscle-specific, housekeeping, and silent genes in undifferentiated and differentiated C2C12 cells to determine whether H3.3 incorporation was altered by differentiation and the activation of myogenic gene expression. At myogenic loci, H3.3 incorporation increased at the TSS and in the gene body upon differentiation, but minimally at the TES (Supplementary Figure S7B). Silent genes showed no H3.3 incorporation upon differentiation, and housekeeping genes showed an increase at the TSS (Supplementary Figure S7C and D). These data indicate that despite the incorporation of H3.3 across myogenic loci in undifferentiated cells, H3.3 incorporation was further increased upon differentiation and the activation of myogenic gene expression.

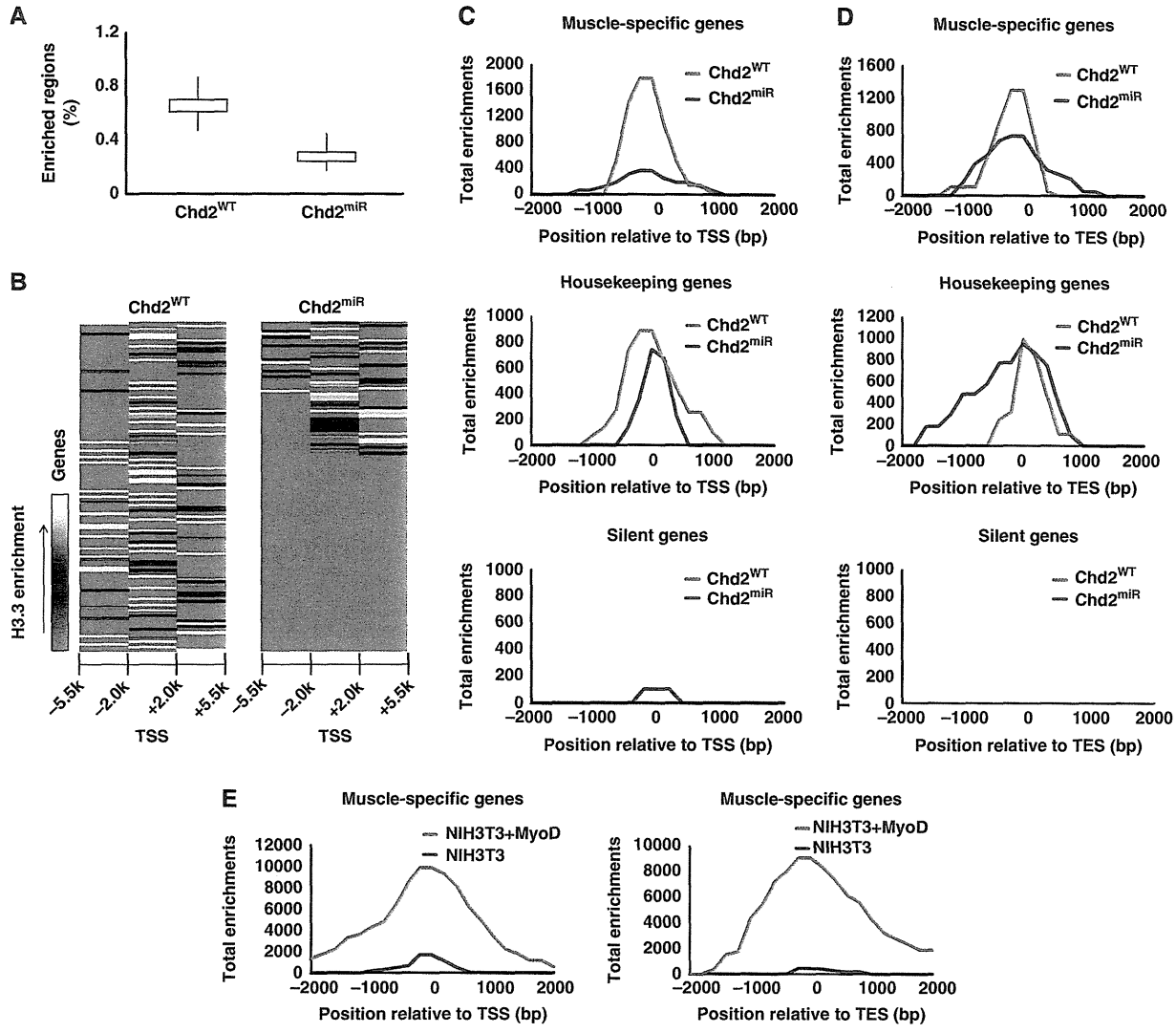

Figure 7 Knockdown of Chd2 decreases the incorporation of H3.3 into the muscle-specific gene loci on a genome-wide level. (**A**) H3.3 deposition in each chromosome is limited. The box plot represents the range of incorporation of H3.3 into each chromosome. (**B**) Chd2 knockdown changes the deposition of H3.3. The heat map represents the enrichment of H3.3 in upregulated genes during myogenic differentiation at the transcriptional start sites (TSS) ± 5.5 kb. The maximum value of H3.3 enrichment is ~10. Each row represents the enrichment pattern of H3.3 along the ± 5.5 kb relative to the TSS. (**C**, **D**) Incorporation of H3.3 at the TSS and TES of muscle-specific, housekeeping, and silent gene loci in undifferentiated C2C12 cells. The H3.3 enrichment Tags from ChIP-Seq data aligned to the TSS and TES were segregated into 200 bp windows. Total enrichments were tallied in muscle-specific, housekeeping and silent genes (Supplementary Dataset 1). (**E**) MyoD-dependent induction of H3.3 incorporation at the TSS (left panel) and TES (right panel) of skeletal muscle gene loci in fibroblast cells ectopically expressing MyoD. Total enrichments were tallied for muscle-specific genes as in (**C**, **D**).

Deposition of H3.3 at differentiation-specific genes contrasts with deposition of H3.3 at the Myod1 locus

Finally, we directly analysed the requirement of H3.3 for myogenic differentiation. siRNA sequences targeting the two H3.3 genes in mouse cells were introduced into C2C12 cells. MHC staining and myotube formation were absent in the cells depleted for H3.3 (Figure 8A). Expression of representative myogenic genes was also compromised upon H3.3 knockdown (Figure 8B). Western blot analysis demonstrated that H3.3 levels, but not H3.1 levels were reduced under both growth and differentiation conditions (Figure 8C).

The data from the H3.3 knockdown experiment is consistent with that from a previous publication that used cells expressing epitope-tagged H3.3 to demonstrate H3.3 incorporation at the locus encoding MyoD (*Myod1*). Specifically, H3.3 incorporation was shown in the proximal regulatory region (PRR) of the *Myod1* locus, 200 bp upstream of the transcription start site, as differentiation proceeded. However, those authors determined that H3.3 incorporation at *Myod1* was dependent on the histone chaperones, HIRA and Asf1a, whereas it was independent of Asf1b and Chd1 (Yang *et al*, 2011). To further investigate, we compared H3.3 incorporation at differentiation-specific genes such as *Acta1* and *Myog* with *Myod1* PRR in undifferentiated cells. Consistent with the results presented above, knockdown of Chd2 prevented H3.3 incorporation at *Acta1* and *Myog* (Figure 8D). Chd2 knockdown had no effect on H3.3 incorporation at the *Myod1* sequence or at the housekeeping genes. Interestingly, H3.3 knockdown prevented H3.3

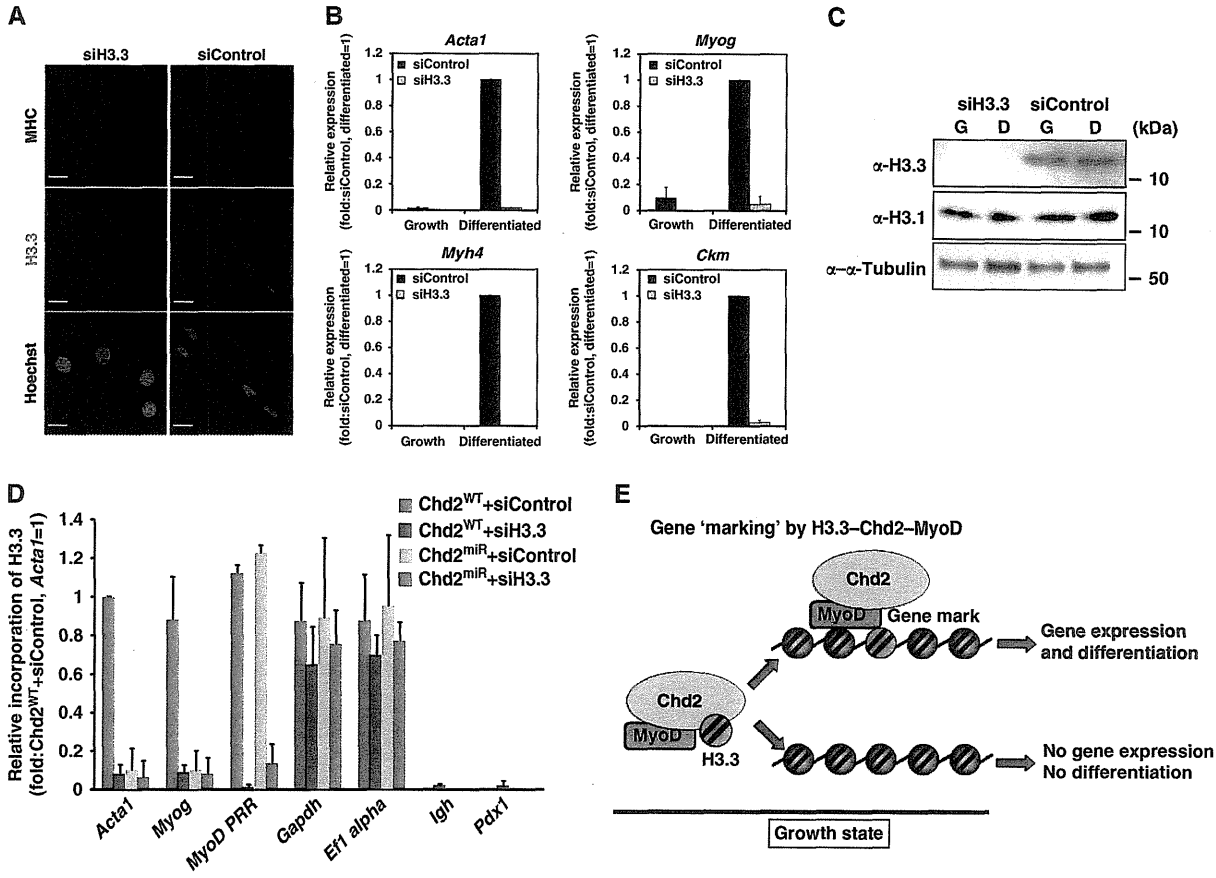

Figure 8 H3.3 is required for myogenic differentiation. (**A**) The expression of myosin heavy chain (MHC; red) and myotube formation was not induced in C2C12 cells when H3.3 expression was suppressed by siRNAs targeting *H3f3a* and *H3f3b*. Scale bars = 5 μm. (**B**) The transcription of skeletal muscle marker genes was suppressed in C2C12 cells expressing siRNAs targeting *H3f3a* and *H3f3b*. mRNA levels were analysed by Q-PCR; data represent the average of three independent experiments ± s.d. (**C**) Western blot evaluating H3.3 protein knockdown and the expression of the other indicated proteins. (**D**) siRNA-mediated H3.3 knockdown inhibits H3.3 recruitment onto *Acta1*, *Myog* and *Myod1*, while in Chd2 knockdown cells, H3.3 incorporation is not decreased at *Myod1*. ChIP assays were performed as in Figure 6. (**E**) Schematic representation of the 'marking' of myogenic genes by Chd2 prior to myogenesis. Chd2 coordinates with MyoD to direct H3.3 to differentiation-dependent, skeletal muscle-specific gene loci during the growth state. Incorporation of H3.3 marks myogenic loci for expression following the initiation of the differentiation process.

incorporation at the myogenic sequences tested but did not affect H3.3 incorporation at the housekeeping genes (Figure 8D). Though the reasons remain to be explored, this result suggests that under conditions of H3.3 depletion, incorporation of the remaining H3.3 is non-random. Regardless, these data, coupled with the earlier report (Yang *et al*, 2011) clearly demonstrate that the mechanisms controlling deposition of H3.3 at the *Myod1* locus differ from those controlling H3.3 incorporation at downstream myogenic genes activated upon differentiation.

In summary, our directed and genome-wide profiling of H3.3 incorporation provides a mechanism accounting for the inhibition of myogenesis caused by knockdown of Chd2. A schematic drawing outlining Chd2-dependent deposition of H3.3 to mark differentiation-specific genes prior to the onset of differentiation and differentiation-specific gene expression is presented in Figure 8E.

Discussion

We showed that Chd2-mediated H3.3 deposition helps determine the gene expression programme for skeletal muscle differentiation. Our results suggest that Chd2 participates in selecting whether a gene will be expressed during muscle differentiation via its localization to myogenic gene loci in the undifferentiated state. The selected gene is then marked for expression by Chd2-dependent incorporation of H3.3 into the gene locus. The presence of the H3.3 variant in chromatin is associated with histone modifications that generally signal transcriptionally poised or transcriptionally competent chromatin (Wirbelauer *et al*, 2005; Hake *et al*, 2006; Goldberg *et al*, 2010) and has been proposed to be associated with epigenetic memory (Hake and Allis, 2006; Ng and Gurdon, 2008). Thus, the deposition of H3.3 at myogenic genes in myoblast cells represents a mechanism by which differentiation-specific genes can be marked for activation once differentiation signalling induces the onset of myogenesis.

The enzymatic activities of Chd2 are not well characterized. Analysis of Chd2 mutant mice indicated that Chd2 plays a critical role in development and tumour suppression (Marfella *et al*, 2006; Nagarajan *et al*, 2009). Moreover, Chd2 appears to be ubiquitously expressed, though highly enriched in muscle tissues (Marfella *et al*, 2006). The closely

related Chd1 enzyme, however, has been shown to incorporate H3.3 into nucleosomes in a Hira-independent manner (Konev *et al*, 2007). CHD1 also binds to the K4me3 mark associated with the activation of gene expression (Sims *et al*, 2005), and Chd1 is essential for maintaining pluripotency in ES cells (Gaspar-Maia *et al*, 2009). Despite the structural similarity of the Chd1 and Chd2 proteins, they do not appear to be redundant, because the data presented here indicates that in undifferentiated and differentiated cells, Chd2, but not Chd1, interacts with MyoD and that Chd2 associates with H3.3 with greater frequency than does Chd1. The functional relationship between these two structurally related proteins remains to be determined.

The ChIP-Seq analysis of H3.3 using next-generation sequencing represents the first analysis of endogenous H3.3 incorporation into chromatin in any genome. The data indicate that H3.3 incorporation is extremely limited across the myoblast genome, and is concentrated at both the TSS and the TES of transcribed genes. The localization of H3.3 is not surprising; earlier studies of epitope-tagged H3.3 also revealed that it localizes near the TSS and TES of actively transcribed genes (Jin *et al*, 2009). The significance of localization to TES of active genes is not presently understood. Unexpectedly, the data indicate that knockdown of Chd2 not only reduced H3.3 incorporation at some genes but also showed enhanced incorporation at other genes. This might indicate that Chd2 both positively and negatively regulates incorporation of H3.3 across the genome. Alternatively, or in addition, other proteins that can modulate H3.3 incorporation (Yang *et al*, 2011) may have altered activities or altered targets upon misregulation of Chd2 levels.

We found that Chd2 specifically associates with MyoD in the undifferentiated state by three distinct methods: co-IP, co-localization by immunofluorescence, and PLA. Although we did not perform the co-IP experiment in differentiated cells, we did utilize the co-immunofluorescence and PLA assays to demonstrate that the MyoD–Chd2 interaction remains during differentiation. The MyoD-related protein Myf5 can compensate for the function of MyoD; however, we were unable to assess whether Myf5 could bind Chd2 or to Chd2 target genes as we were unable to identify an antibody that could reliably immunoprecipitate Myf5. While we cannot exclude the possibility that Myf5 also contributes to Chd2 function, the data presented suggest that MyoD is required for Chd2 binding to and for Chd2-dependent deposition of H3.3 at myogenic sequences.

Though gene-specific evidence for MyoD binding to target genes before differentiation is limited (Mal and Harter, 2003), a genomic analysis of MyoD binding in C2C12 myoblasts indicates that MyoD is bound widely throughout the genome, including at most myogenic genes (Cao *et al*, 2010). These findings provide a mechanism to explain the selective targeting of Chd2 to myogenic genes in the undifferentiated state. Once marked by incorporation of H3.3, the gene is ready to be transcribed upon differentiation signalling, which results in numerous molecular changes at myogenic regulatory sequences and throughout these loci (Tapscott, 2005; Keren *et al*, 2006).

The data presented here demonstrate that differentiation-specific myogenic genes are marked by incorporation of the H3.3 histone variant in a manner dependent upon MyoD and the Chd2 enzyme. This contrasts with deposition of H3.3 at the *Myod1* locus (Yang *et al*, 2011), which is independent of Chd2 but is consistent with the idea that MyoD itself is expressed prior to differentiation. These marks occur prior to the onset of differentiation and gene expression, and the absence of these marks precludes myogenic gene expression. Thus, the MyoD–Chd2–H3.3 axis provides a novel mechanism for potentiating the expression of differentiation-specific genes upon subsequent differentiation signalling.

Materials and methods

Cells

C2C12 cells were cultured in Dulbecco's modified Eagle's medium (DMEM) supplemented with 20% fetal bovine serum. Cells examined under growth conditions were harvested at 60–70% confluency. Differentiated samples were transferred to DMEM containing 2% horse serum upon reaching confluence and harvested 48 h later. The NIH3T3-derived cell (B22) line was infected with retrovirus expressing MyoD as described previously (de la Serna *et al*, 2001).

miRNA expression constructs

The oligonucleotides used for expression of *Chd2* and for the negative control (*lacZ*) miRNAs are described in Supplementary Table SI. Annealed oligonucleotides were ligated into pT2A-CAG/EGFP-NLS, which contains TolII transposon elements and EGFP-NLS cDNA located upstream of the miRNA sequence and which was modified from pT2AL200R150G (Kawakami and Noda, 2004; Kawakami *et al*, 2004; Urasaki *et al*, 2006).

Plasmid transfection and cell line selection

The pT2A-CAG/EGFP-NLS-miRNA transfection was performed using Gene Juice transfection 2 reagent (Novagen). C2C12 cells at 20–30% confluence were transfected with a miRNA expression vector (6 μg plasmid DNA per 100-mm plate), pCAGGS-TP coding transposase (provided by Dr Kawakami), and pT2A-CAG/puromycin and incubated for 24 h. To create cell lines stably expressing miRNAs targeting *Chd2*, we transfected cells with four distinct candidate miRNAs (Supplementary Table SI). To create a control line, cells were transfected with a miRNA against *lacZ*. Transfected cells were cultured for 7 days in the presence of 2 μg/ml puromycin. From the four pools of transfectants, we selected the two ($Chd2^{miR3139}$, $Chd2^{miR5111}$) that showed the greatest suppression of Chd2 expression. We then created single cell clones from each pool, as well as from the control ($Chd2^{WT}$) pool, by dilution such that one cell was plated per every 24 wells of a 96-well plate. Four monoclonal lines were chosen from each of the original pools based on the extent of the Chd2 knockdown. All four $Chd2^{miR3139}$ clones and all four $Chd2^{miR5111}$clones showed suppression of Chd2 expression, inhibition of myogenic gene expression, and inhibition of myotube formation when differentiation was induced. All four of the $Chd2^{WT}$ clones showed no change in Chd2 expression compared with parental C2C12 cells and showed no change in myogenic expression or myotube formation when induced to differentiate. One of each clone for $Chd2^{miR3139}$, $Chd2^{miR5111}$, and $Chd2^{WT}$ was chosen for further study. All experiments were completed with cell lines that were passaged 10 times or less.

Rescue experiments

Each competitive mRNA fragment (*Chd2*-3011-3283, *Chd2*-5004-5177) was ligated downstream of the mKO1-NLS mRNA in the pT2A/CAG expression vector. Stable transfection was performed to introduce both the *Chd2*-targeting miRNA and the competitive mRNA fragment as indicated.

Each cDNA (*Chd2* full-length or *Chd2*(Δ281–512 aa)) was ligated downstream of the mKO2 mRNA in the Bidirectional Tet Expression Vector pTETmKO2 (Clontech Tet-On system and (Sakaue-Sawano *et al*, 2008)). Stable transfection was performed to introduce both the *Chd2*-targeting miRNA and the indicated *Chd2* cDNA.

Monoclonal antibodies

The Chd1, Chd2, MyoD, Brm, and Brg1 rat monoclonal antibodies were described (Ohkawa *et al*, 2009; Okada *et al*, 2009; Harada *et al*, 2010a, b; Yoshimura *et al*, 2010). The H3.3 and H3.1 antigens were

synthesized based on their specific sequences, H3.3: CATKAARKSA PSTGGVKKPH (AA 21–39) and H3.1: CATKAARKSAPATGGVKKPH (AA 21–39 aa) (Sigma-Aldrich). The N-terminal cysteine residue allowed coupling to maleimide-activated keyhole limpet haemocyanin (Thermo Scientific), a carrier protein. The coupling reaction followed the instructions provided the supplier. Rat (H3.3) or mouse (H3.1) monoclonal antibodies were generated based on the lymph node method established by Sado *et al* (1995)(Kishiro *et al*, 1995). In all, 200 μg H3.3 or H3.1 peptide was used as antigen. Hybridoma cells were cloned in HAT selection medium (hybridoma SFM medium (Invitrogen); 10% fetal bovine serum; 10% BM-Condimed H1 (Roche); 100 μM hypoxanthine; 0.4 μM aminopterin; 1.6 μM thymidine) and were screened 7 days post-fusion using an enzyme-linked immunoadsorbent assay (ELISA) against each antigen. H3.3-positive clone specificity was confirmed by checking cross-reactivity for the H3.1 peptide and H3.1-positive clone specificity was confirmed by checking cross-reactivity for the H3.3 peptide. Positive clones were subcloned and rescreened by ELISA. Concentrated antibody preparations were made from clones 4H2D7 (for H3.3) and 1D4F2 (for H3.1) that were cultured at high density using a miniPERM bioreactor (Vivascience).

ELISA

BSA-conjugated H3.3 or H3.1 peptide (5 μg/ml) was diluted from 1:100 to 1:100 000 in 10 mM sodium phosphate pH 7.0 and then adsorbed on Costar Serocluster 96-Well 'U' Bottom Plates (Corning) at 4°C for 12–24 h. The plates were subsequently blocked with 1% BSA in PBS to prevent non-specific associations. Hybridoma supernatants were applied for 1 h at room temperature followed by three PBS washes and then 30 min incubation at room temperature with alkaline phosphatise-conjugated anti-rat or anti-mouse IgG antibody (Sigma) diluted to 1:10 000. Immunoreactivity was identified by a pNPP phosphatase substrate system (KPL) after washing with TBS-T three times.

Immunoprecipitation, immunoblotting, and ICC

IP, western blot analysis, and ICC were performed as described (Harada *et al*, 2010b). For IP, cleared lysates were rocked with 10 μl of rabbit antisera against MyoD (de la Serna *et al*, 2005) or 100 μl supernatant of monoclonal antibody against Chd2 (ascites, 8H3) for 12 h. For immunoblotting, primary antibodies used included rabbit anti-MyoD (C-20, Santa Cruz Biotechnology, 1:1000; Figure 1A only), anti-cyclin A (C-19, Santa Cruz Biotechnology, 1:1000), anti-cyclin E (M-20, Santa Cruz Biotechnology, 1:1000), anti-α-tubulin (Cell Signaling, 1:2000), anti-H3 (Cell Signaling, 1:1000), mouse anti-GFP (GF200, Nacalai Tesque, 1:500), rat anti-Chd2 (8H3, hybridoma supernatant, 1:100), anti-H3.3 (hybridoma supernatant, 1:1000), anti-H3.1 (hybridoma supernatant, 1:1000), anti-MyoD (hybridoma supernatant, 1:100), and anti-Chd1 (hybridoma supernatant, 1:1000). Secondary antibodies were horseradish peroxidase-conjugated anti-rabbit, anti-mouse, or anti-rat IgG antibodies (1:5000; GE Healthcare). For ICC, 1% paraformaldehyde was used for fixation. Primary antibodies included rat monoclonal anti-Chd2 (8H3, hybridoma supernatant, 1:50), anti-Chd1 (2F11, hybridoma supernatant, 1:100), anti-H3.3 (4H2D7, hybridoma supernatant, 1:2), rabbit anti-myosin heavy chain (Calbiochem, 1:100), anti-Myogenin (M-225, Santa Cruz Biotechnology, 1:500), or anti-MyoD (C-20, Santa Cruz Biotechnology, 1:200), mouse anti-H3K4me3 (gifted from Dr H Kimura, 1:1000) (Kimura *et al*, 2008), anti-H3K9me2 (gifted from Dr H Kimura, 1:1000) (Hayashi-Takanaka *et al*, 2011). Images were visualized using a confocal microscope (LSM510; Carl Zeiss). Co-localization was evaluated by ImageJ (NCBI). Co-localization frequency was analysed as described previously (vanSteensel *et al*, 1996), except that the cross-correlation function was calculated by rotating the red image (labelling Alexa-588) over an angle $x°$ in the x orientation with respect to the green image (labelling Alexa-488) such as $-90 = x = 90$. A negative value of x indicates that the red image was rotated counterclockwise, and a positive value indicates a clockwise rotation. Pearson's correlation coefficient (γ_p) was calculated for each value of x and plotted against x to obtain the cross-correlation function (vanSteensel *et al*, 1996).

Proximity ligation assay

Proximity ligation was performed using a Duolink assay kit II (OlinkBiosciences) according to the protocol provided by manufacturer, except that the oligonucleotide-conjugated anti-rabbit probe was used at 1:20 and the anti-rat probe conjugated by probemaker was used at 1:40. Finally, the coverslips were again mounted with Duolink Mounting Medium contained Bisbenzimide H33342 Fluorochrome Trihydrochloride (Hoechst). All images were taken with an epifluorescence microscope (BX51; Olympus) with ×40 objective and analysed with NIH ImageJ software. Three images were taken from each sample. Antibodies used included the affinity purified rabbit anti-MyoD (de la Serna *et al*, 2005) and rat monoclonals against Brg1 and Chd2 (Ohkawa *et al*, 2009; Harada *et al*, 2010b) for Figure 1D and 1E. In Figure 5, the rat H3.3 and mouse H3.1 monoclonals described above were used with affinity purified rabbit antibody generated against the Chd2 antigen described previously (Harada *et al*, 2010b).

Quantitative RT–PCR

Total RNA was isolated and reversed-transcribed with Takara Prime Script Reverse Transcriptase and an oligo dT primer as described (Valdez *et al*, 2000). Q-PCR was performed using TaKaRa SYBR Premix Dimer Eraser and primers listed in Supplementary Table SII. Q-PCR data are presented as mean ± s.d. of three independent experiments.

Fluorescence-activated cell sorting (FACS)

FACS analysis of propidium iodide-stained cells was performed as described (Dacwag *et al*, 2007).

siRNA-mediated knockdown of MyoD, Chd2, and H3.3

Knockdown of MyoD, Chd2, H3.3 was performed by transfection of the C2C12 cells with siRNA duplex oligos (Kumar *et al*, 2003; Yang *et al*, 2011) using Lipofectamine RNAiMAX (Invitrogen) according to the manufacturer's protocol. Control RNAi (Mission_Negative control SIC-001; proprietary sequence), MyoD-RNAi: (5′-GGCCUG UCAAGUCUAUGUC-3′ and 5′-GGCAUAGACUUGACAGGCC-3′), H3f3a-RNAi: (5′-GAGAAAUUG CUC AGGACU UTT-3′ and 5′-AAG UCCUGAGCAAUUUCUCTT-3′), H3f3b-RNAi: (5′-CAGAGAUUG GUG AGGGAGA TT-3′ and 5′-UCUCCCUCACCAAUCUCUGTT-3′) were synthesized by Sigma. Chd2-RNAi: (5′-AAAUCCUGCUGGUGAUA AUUCUGGG-3′ and 5′-CCCAGAAUUAUCACCAGCAGGAUUU-3′) were synthesized by Invitrogen.

Chromatin immunoprecipitation

ChIP assays were performed by modifying the Upstate Biotechnology protocol as described previously (Dacwag *et al*, 2007) utilizing the rat monoclonal antibodies against Chd2 (8H3, ascites, 20 μl) and H3.3 (4H2D7, ascites, 20 μl). Relative recruitment or incorporation was defined as the ratio of amplification of the PCR product relative to 1% of input genomic DNA. Quantification represents the mean of three independent experiments ± s.d. ChIP experiments using IgG were performed as controls (Supplementary Figure S8). The primers used to amplify the promoter regions are listed in Supplementary Table SIII. Re-ChIP assays were performed as described previously (Ohkawa *et al*, 2006).

ChIP-seq and data analysis

Sample preparation was performed as described above except cells were not fixed. The ChIP library was prepared with the Illumina protocol and sequencing analysis was performed using the Genome Analyser GAIIx (Illumina KK). The base-called sequences were obtained using SCS2.7 from ChIP-seq image data. The sequence tags for H3.3 and Input were aligned to the mouse genome (mm9) using ELAND v2, BWA (Li and Durbin, 2009), and Bowtie (Langmead *et al*, 2009) software. We adapted the alignment data of Bowtie so that the alignment efficiency was optimized. Unique tag numbers are listed in Supplementary Table SIV. Peak detection and identification of binding sites of H3.3 were obtained by correcting from Input DNA using MACS (Zhang *et al*, 2008) with default parameters except bw = 300 based on the fragmented size of the ChIP sample. The calculated FDR was ⩽0.1%. The box plot of H3.3-enriched regions was obtained giving the sum total of the enrichment area (bp) of H3.3, found in MACS, of each chromosome divided by the length (bp) of each chromosome. The heat map was generated from H3.3 enrichment of the genes that were upregulated after induction of skeletal muscle differentiation (Supplementary Dataset 1), based on the microarray analysis in C2C12 cells (Tomczak *et al*, 2004). The maximum value of H3.3 enrichment is ~10. Each row represents the enrichment pattern of H3.3 along the

±5.5 kb relative to the TSS. The total enrichments of TSS/TES ±2 kb obtained by the H3.3 enrichment Tags aligned at TSS/TES that were segregated into 200 bp windows were tallied for skeletal muscle-specific genes, housekeeping genes and silent genes in C2C12 cells, based on published microarray analyses in C2C12 cells, NIH3T3 cells, and RAW264.7 cells (Tomczak *et al*, 2004; Berenjeno *et al*, 2007; Covert *et al*, 2009). Microarray data were obtained from NCBI GEO GSM137347(NIH3T3), GSE989(C2C12), GSM197840(RAW264.7). All defined gene lists are shown in Supplementary Dataset 1. Reference gene annotation was determined using the UCSC genome browser (http://genome.ucsc.edu).

Accession numbers

ChIP-seq data were deposited with accession codes DRA000164, DRA000165, DRA000166, DRA000218, and DRA000219 (DNA Data Bank of Japan).

Supplementary data

Supplementary data are available at *The EMBO Journal* Online (http://www.embojournal.org).

Acknowledgements

We thank Dr K Kawakami for providing plasmids; Dr Kimura for providing monoclonal antibodies; Dr K Maeshima for advice; and Mr Maehara, Ms Ichinose, Itoh, Koga, Miharu, and Onishi for technical support. This work was supported in part by grants from the Ministry of Education, Culture, Sports, Science, and Technology of Japan, the Kaibara Morikazu Medical Science Promotion Foundation, and by NIH Grant GM56244.

Author contributions: AH designed and performed the experiments and wrote the manuscript. SO contributed ideas and interpreted the results. DK performed the experiments related to miRNA expression. JO performed the immunoprecipitation experiments. TY, SY, and T Tachibana established and characterised rat monoclonal antibodies. H Kumamaru, HS, and T Tsubota interpreted the results. H Kurumizaka provided recombinant H3.1 and H3.3 proteins. KA interpreted the results. ANI contributed ideas, interpreted the results, and wrote the manuscript. YO designed the project, designed experiments, contributed ideas, interpreted results, and wrote the manuscript.

Conflict of interest

The authors declare that they have no conflict of interest.

References

Ahmad K, Henikoff S (2002) The histone variant H3.3 marks active chromatin by replication-independent nucleosome assembly. *Mol Cell* **9:** 1191–1200

Berenjeno IM, Nunez F, Bustelo XR (2007) Transcriptomal profiling of the cellular transformation induced by Rho subfamily GTPases. *Oncogene* **26:** 4295–4305

Cao Y, Yao Z, Sarkar D, Lawrence M, Sanchez GJ, Parker MH, MacQuarrie KL, Davison J, Morgan MT, Ruzzo WL, Gentleman RC, Tapscott SJ (2010) Genome-wide MyoD binding in skeletal muscle cells: a potential for broad cellular reprogramming. *Dev Cell* **18:** 662–674

Covert J, Mathison AJ, Eskra L, Banai M, Splitter G (2009) Brucella melitensis, B. neotomae and B. ovis elicit common and distinctive macrophage defense transcriptional responses. *Exp Biol Med (Maywood)* **234:** 1450–1467

Dacwag CS, Ohkawa Y, Pal S, Sif S, Imbalzano AN (2007) The protein arginine methyltransferase Prmt5 is required for myogenesis because it facilitates ATP-dependent chromatin remodeling. *Mol Cell Biol* **27:** 384–394

Davis RL, Weintraub H, Lassar AB (1987) Expression of a single transfected CDNA converts fibroblasts to myoblasts. *Cell* **51:** 987–1000

de la Serna IL, Carlson KA, Imbalzano AN (2001) Mammalian SWI/SNF complexes promote MyoD-mediated muscle differentiation. *Nature Genet* **27:** 187–190

de la Serna IL, Ohkawa Y, Berkes CA, Bergstrom DA, Dacwag CS, Tapscott SJ, Imbalzano AN (2005) MyoD targets chromatin remodeling complexes to the myogenin locus prior to forming a stable DNA-bound complex. *Mol Cell Biol* **25:** 3997–4009

Garcia BA, Pesavento JJ, Mizzen CA, Kelleher NL (2007) Pervasive combinatorial modification of histone H3 in human cells. *Nat Methods* **4:** 487–489

Gaspar-Maia A, Alajem A, Polesso F, Sridharan R, Mason MJ, Heidersbach A, Ramalho-Santos J, McManus MT, Plath K, Meshorer E, Ramalho-Santos M (2009) Chd1 regulates open chromatin and pluripotency of embryonic stem cells. *Nature* **460:** 863–U897

Goldberg AD, Banaszynski LA, Noh KM, Lewis PW, Elsaesser SJ, Stadler S, Dewell S, Law M, Guo XY, Li X, Wen DC, Chapgier A, DeKelver RC, Miller JC, Lee YL, Boydston EA, Holmes MC, Gregory PD, Greally JM, Rafii S *et al* (2010) Distinct factors control histone variant H3.3 localization at specific genomic regions. *Cell* **140:** 678–691

Hake SB, Allis CD (2006) Histone H3 variants and their potential role in indexing mammalian genomes: the 'H3 barcode hypothesis'. *Proc Natl Acad Sci USA* **103:** 6428–6435

Hake SB, Garcia BA, Duncan EM, Kauer M, Dellaire G, Shabanowitz J, Bazett-Jones DP, Allis CD, Hunt DF (2006) Expression patterns and post-translational modifications associated with mammalian histone H3 variants. *J Biol Chem* **281:** 559–568

Harada A, Ohkawa Y, Ao S, Odawara J, Okada S, Azuma M, Nishiyama Y, Nakamura M, Tachibana T (2010a) Rat monoclonal antibody specific for MyoD. *Hybridoma (Larchmt)* **29:** 255–258

Harada A, Yoshimura S, Odawara J, Azuma M, Okada S, Nakamura M, Tachibana T, Ohkawa Y (2010b) Generation of a rat monoclonal antibody specific for CHD2. *Hybridoma (Larchmt)* **29:** 173–177

Hayashi-Takanaka Y, Yamagata K, Wakayama T, Stasevich TJ, Kainuma T, Tsurimoto T, Tachibana M, Shinkai Y, Kurumizaka H, Nozaki N, Kimura H (2011) Tracking epigenetic histone modifications in single cells using Fab-based live endogenous modification labeling. *Nucleic Acids Res* **39:** 6475–6488

Jin CY, Zang CZ, Wei G, Cui KR, Peng WQ, Zhao KJ, Felsenfeld G (2009) H3.3/H2A.Z double variant-containing nucleosomes mark 'nucleosome-free regions' of active promoters and other regulatory regions. *Nat Genet* **41:** 941–U112

Karasawa S, Araki T, Nagai T, Mizuno H, Miyawaki A (2004) Cyan-emitting and orange-emitting fluorescent proteins as a donor/acceptor pair for fluorescence resonance energy transfer. *Biochem J* **381:** 307–312

Kawakami K, Noda T (2004) Transposition of the Tol2 element, an Ac-like element from the Japanese medaka fish Oryzias latipes, in mouse embryonic stem cells. *Genetics* **166:** 895–899

Kawakami K, Takeda H, Kawakami N, Kobayashi M, Matsuda N, Mishina M (2004) A transposon-mediated gene trap approach identifies developmentally regulated genes in zebrafish. *Dev Cell* **7:** 133–144

Keren A, Tamir Y, Bengal E (2006) The p38 MAPK signaling pathway: A major regulator of skeletal muscle development. *Mol Cell Endocrinol* **252:** 224–230

Kimura H, Hayashi-Takanaka Y, Goto Y, Takizawa N, Nozaki N (2008) The organization of histone H3 modifications as revealed by a panel of specific monoclonal antibodies. *Cell Struct Function* **33:** 61–73

Kishiro Y, Kagawa M, Naito I, Sado Y (1995) A novel method of preparing rat-monoclonal antibody-producing hybridomas by using rat medial iliac lymph-node cells. *Cell Struct Function* **20:** 151–156

Konev AY, Tribus M, Park SY, Podhraski V, Lim CY, Emelyanov AV, Vershilova E, Pirrotta V, Kadonaga JT, Lusser A, Fyodorov DV (2007) CHD1 motor protein is required for deposition of histone variant h3.3 into chromatin *in vivo*. *Science* **317:** 1087–1090

Kouskouti A, Talianidis I (2005) Histone modifications defining active genes persist after transcriptional and mitotic inactivation. *EMBO J* **24:** 347–357

Kumar R, Conklin DS, Mittal V (2003) High-throughput selection of effective RNAi probes for gene silencing. *Genome Res* **13:** 2333–2340

Langmead B, Trapnell C, Pop M, Salzberg SL (2009) Ultrafast and memory-efficient alignment of short DNA sequences to the human genome. *Genome Biol* **10:** R25

Li H, Durbin R (2009) Fast and accurate short read alignment with Burrows-Wheeler transform. *Bioinformatics* **25:** 1754–1760

Mal A, Harter ML (2003) MyoD is functionally linked to the silencing of a muscle-specific regulatory gene prior to skeletal myogenesis. *Proc Natl Acad Sci USA* **100:** 1735–1739

Marfella CGA, Ohkawa Y, Coles AH, Garlick DS, Jones SN, Imbalzano AN (2006) Mutation of the SNF2 family member Chd2 affects mouse development and survival. *J Cell Physiol* **209:** 162–171

Meshorer E, Yellajoshula D, George E, Scambler PJ, Brown DT, Mistell T (2006) Hyperdynamic plasticity in pluripotent embryonic of chromatin proteins stem cells. *Dev Cell* **10:** 105–116

Nagarajan P, Onami TM, Rajagopalan S, Kania S, Donnell R, Venkatachalam S (2009) Role of chromodomain helicase DNA-binding protein 2 in DNA damage response signaling and tumorigenesis. *Oncogene* **28:** 1053–1062

Ng RK, Gurdon JB (2008) Epigenetic memory of an active gene state depends on histone H3.3 incorporation into chromatin in the absence of transcription. *Nat Cell Biol* **10:** 102–U183

Ohkawa Y, Harada A, Nakamura M, Yoshimura S, Tachibana T (2009) Production of a rat monoclonal antibody against Brg1. *Hybridoma (Larchmt)* **28:** 463–466

Ohkawa Y, Marfella CGA, Imbalzano AN (2006) Skeletal muscle specification by myogenin and Mef2D via the SWI/SNF ATPase Brg1. *EMBO J* **25:** 490–501

Okada S, Harada A, Saiwai H, Nakamura M, Ohkawa Y (2009) Generation of a Rat Monoclonal Antibody Specific for Brm. *Hybridoma* **28:** 455–458

Okano M, Bell DW, Haber DA, Li E (1999) DNA methyltransferases Dnmt3a and Dnmt3b are essential for *de novo* methylation and mammalian development. *Cell* **99:** 247–257

Pray-Grant MG, Daniel JA, Schieltz D, Yates JR, Grant PA (2005) Chd1 chromodomain links histone H3 methylation with SAGA- and SLIK-dependent acetylation. *Nature* **433:** 434–438

Ray-Gallet D, Quivy JP, Scamps C, Martini EMD, Lipinski M, Almouzni G (2002) HIRA is critical for a nucleosome assembly pathway independent of DNA synthesis. *Mol Cell* **9:** 1091–1100

Sado Y, Kagawa M, Kishiro Y, Sugihara K, Naito I, Seyer JM, Sugimoto M, Oohashi T, Ninomiya Y (1995) Establishment by the rat lymph-node method of epitope-defined monoclonal-antibodies recognizing the 6 different alpha-chains of human Type-Iv collagen. *Histochem Cell Biol* **104:** 267–275

Sakaue-Sawano A, Kurokawa H, Morimura T, Hanyu A, Hama H, Osawa H, Kashiwagi S, Fukami K, Miyata T, Miyoshi H, Imamura T, Ogawa M, Masai H, Miyawaki A (2008) Visualizing spatiotemporal dynamics of multicellular cell-cycle progression. *Cell* **132:** 487–498

Simone C, Forcales SV, Hill DA, Imbalzano AN, Latella L, Puri PL (2004) p38 pathway targets SWI-SNF chromatin-remodeling complex to muscle-specific loci. *Nat Genet* **36:** 738–743

Sims RJ, Chen CF, Santos-Rosa H, Kouzarides T, Patel SS, Reinberg D (2005) Human but not yeast CHD1 binds directly and selectively to histone H3 methylated at lysine 4 via its tandem chromodomains. *J Biol Chem* **280:** 41789–41792

Takahashi K, Yamanaka S (2006) Induction of pluripotent stem cells from mouse embryonic and adult fibroblast cultures by defined factors. *Cell* **126:** 663–676

Tapscott SJ (2005) The circuitry of a master switch: Myod and the regulation of skeletal muscle gene transcription. *Development* **132:** 2685–2695

Tomczak KK, Marinescu VD, Ramoni MF, Sanoudou D, Montanaro F, Han M, Kunkel LM, Kohane IS, Beggs AH (2004) Expression profiling and identification of novel genes involved in myogenic differentiation. *FASEB J* **18:** 403–405

Tontonoz P, Hu ED, Spiegelman BM (1994) Stimulation of adipogenesis in fibroblasts by Ppar-Gamma-2, a lipid-activated transcription factor. *Cell* **79:** 1147–1156

Urasaki A, Morvan G, Kawakami K (2006) Functional dissection of the Tol2 transposable element identified the minimal cis-sequence and a highly repetitive sequence in the subterminal region essential for transposition. *Genetics* **174:** 639–649

Valdez MR, Richardson JA, Klein WH, Olson EN (2000) Failure of Myf5 to support myogenic differentiation without myogenin, MyoD, and MRF4. *Dev Biol* **219:** 287–298

vanSteensel B, vanBinnendijk EP, Hornsby CD, vanderVoort HTM, Krozowski ZS, deKloet ER, vanDriel R (1996) Partial colocalization of glucocorticoid and mineralocorticoid receptors in discrete compartments in nuclei of rat hippocampus neurons. *J Cell Sci* **109:** 787–792

Wirbelauer C, Bell O, Schubeler D (2005) Variant histone H3.3 is deposited at sites of nucleosomal displacement throughout transcribed genes while active histone modifications show a promoter-proximal bias. *Genes Dev* **19:** 1761–1766

Yang JH, Song Y, Seol JH, Park JY, Yang YJ, Han JW, Youn HD, Cho EJ (2011) Myogenic transcriptional activation of MyoD mediated by replication-independent histone deposition. *Proc Natl Acad Sci USA* **108:** 85–90

Yoshimura S, Harada A, Odawara J, Azuma M, Okada S, Nakamura M, Ohkawa Y, Tachibana T (2010) Rat monoclonal antibody specific for the chromatin remodelling factor, CHD1. *Hybridoma (Larchmt)* **29:** 237–240

Zhang Y, Liu T, Meyer CA, Eeckhoute J, Johnson DS, Bernstein BE, Nussbaum C, Myers RM, Brown M, Li W, Liu XS (2008) Model-based analysis of ChIP-Seq (MACS). *Genome Biol* **9:** R137